



Amidoxime functionalization of a poly(acrylonitrile)/silica composite for the sorption of Ga(III) – Application to the treatment of Bayer liquor

Siming Lu, Lifeng Chen, Mohammed Hamza, Chunlin He, Xinpeng Wang,
Yuezhou Wei, Eric Guibal

► To cite this version:

Siming Lu, Lifeng Chen, Mohammed Hamza, Chunlin He, Xinpeng Wang, et al.. Amidoxime functionalization of a poly(acrylonitrile)/silica composite for the sorption of Ga(III) – Application to the treatment of Bayer liquor. *Chemical Engineering Journal*, 2019, 368, pp.459-473. 10.1016/j.cej.2019.02.094 . hal-02428222

HAL Id: hal-02428222

<https://imt-mines-ales.hal.science/hal-02428222>

Submitted on 28 May 2021

HAL is a multi-disciplinary open access archive for the deposit and dissemination of scientific research documents, whether they are published or not. The documents may come from teaching and research institutions in France or abroad, or from public or private research centers.

L'archive ouverte pluridisciplinaire **HAL**, est destinée au dépôt et à la diffusion de documents scientifiques de niveau recherche, publiés ou non, émanant des établissements d'enseignement et de recherche français ou étrangers, des laboratoires publics ou privés.

Amidoxime functionalization of a poly(acrylonitrile)/silica composite for the sorption of Ga(III) – Application to the treatment of Bayer liquor

Siming Lu^a, Lifeng Chen^b, Mohammed F. Hamza^{a,c,d}, Chunlin He^a, Xinpeng Wang^a, Yuezhou Wei^{a,b,*}, Eric Guibal^{d,*}

^a Guangxi Key Laboratory of Processing for Non-ferrous Metals and Featured Materials, School of Resources, Environment and Materials, Guangxi University, Nanning 530004, China

^b School of Nuclear Science and Engineering, Shanghai Jiao Tong University, 800 Dong Chuan Road, Shanghai 200240, China

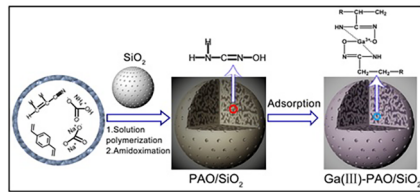
^c Nuclear Materials Authority, POB 530, El-Maadi, Cairo, Egypt

^d C2MA, IMT – Mines Ales, Univ. Montpellier, Alès, France

HIGHLIGHTS

- Successful amidoximation of SiO_2 /polyacrylonitrile composite (SiO_2/PAO).
- PAO/ SiO_2 highly efficient for Ga(III) recovery from slightly acidic solution.
- Ga(III) desorption using 0.5 M HCl solutions for sorbent recycling.
- PAO/ SiO_2 sorbent is selective for Ga(III) recovery from multi-metal solutions.
- Ga(III) efficiently and selectively recovered from Bayer liquor using SiO_2/PAO .

GRAPHICAL ABSTRACT



ABSTRACT

Keywords:
Gallium
Silica core
Poly(acrylamidoxime)
Sorption isotherm
Uptake kinetics
Metal desorption
Sorbent recycling
Bayer liquor

The copolymerization of styrene with divinylbenzene (DVB) in the presence of silica particles produces a commercial silica-supported polymer ($\text{SiO}_2\text{-P}$) that was chemically reacted with acrylonitrile to synthesize silica-supported polyacrylonitrile (PAN/SiO_2). PAN/SiO_2 was functionalized by grafting amidoxime moieties to produce PAO/ SiO_2 sorbent (silica-supported polyacrylamidoxime). The sorbent (PAO/ SiO_2) was characterized by XPS, TGA, FTIR, pH_{pzc} elemental and SEM-EDX analyses and tested for Ga(III) recovery from aqueous solutions. The sorption performance was investigated through the study of pH effect, sorption isotherms at different temperatures, and uptake kinetics under slightly acidic conditions (around pH 4) and at pH close to 13.7 (similar to Bayer liquor). The equilibrium was reached within 60 min; the kinetic profiles can be fitted by the pseudo-second order rate equation (PSORE) and the resistance to intraparticle diffusion equation (RIDE). The maximum sorption capacity reaches 1.34 mmol Ga g⁻¹ at 25 °C (1.76 mmol Ga g⁻¹ at 55 °C); the sorption process is endothermic for solutions prepared by alkaline dissolving of Ga_2O_3 . The sorption capacities are higher for solutions prepared with $\text{Ga}(\text{NO}_3)_3$ salt: the maximum sorption capacity increased up to 2.1–2.6 mmol Ga g⁻¹ (from 25 to 55 °C). Langmuir and Sips equations were used for fitting sorption isotherms. Metal desorption and sorbent recycling were performed using 1.5 M HCl solution. Forty-five minutes were sufficient for achieving complete desorption of Ga(III). Sorption and desorption performances remain stable for a minimum of 5 cycles. Sorbent selectivity for gallium recovery was demonstrated in the presence of an excess of competitor cations. The sorbent was successfully applied for Ga(III) recovery from Bayer liquor at high pH values (around 13): combining relatively high efficiency and selectivity compared with LSC-600 amidoxime resin.

* Corresponding authors.

E-mail addresses: yzwei@gxu.edu.cn (Y. Wei), Eric.Guibal@mines-ales.fr (E. Guibal).

1. Introduction

Gallium is widely applied in high-tech industries, such as optoelectronics and microelectronics for manufacturing high-quality semiconductors, LED lights, mobile phone devices, television and notebook displays, solar cells, and pharmaceutic/radiology drugs [1–5]. Currently, these industrial sectors represent about 80–85% of the total demand on this metal. All these applications in strong expansion require intensive production. Actually, gallium is not extracted from specific mining resources [6], and this metal is only recovered as a by-product of the exploitation of bauxite, vermiculite, coal gangue (as associated mineral), or from high-alumina fly ashes [7,8]. Therefore, it is important to seek an effective way to recover gallium from these secondary resources [9]. Bayer liquor is produced as a result of aluminum leaching from bauxite under pressure and heating; this is one of the most used resource for the extraction of Ga(III).

The most conventional processes for the treatment of Bayer liquor include solvent extraction, electrochemical deposition, fractional precipitation and ion exchange. However, many of these technologies have important drawbacks that hinder their application [10]. For example, the electrochemical deposition method was banned in most countries because of the high toxicity of mercury [11]. The fractional electrolytic process has been basically suspended because of heavy environmental burdens. The Kelex 100 extractant (based on 8-hydroxyquinoline), investigated and patented by Helgorsky and Leveque [12], was used in the solvent extraction process of Bayer liquor as a reaction accelerator [13]. However, the poor cost-effectiveness and the partial dissolution of the extractant in the liquor (which also affects the composition and the extraction performance of the residual solution) have also limited the use of the process. Compared with the above methods, the ion-exchange process appears fast and easy to operate: sodium aluminate can be processed without addition of supplementary reagent. It is commonly accepted that resins currently represent the best for recovering gallium from Bayer liquors.

For the last decades, ion-exchange and chelating resins [14–18] and biosorbents [19,20] have been designed and used for the recovery of toxic and precious metals. For example, silver ions can be recovered using amidoxime/guanidine resins [21]. Kataoka et al. [22] firstly reported that chelating resins that bear both =NOH group and another active group among =NH, –NH₂, –SH or –OH, have a great affinity for gallium. However, they faced various problems, associated, for example, to diffusion properties, which limited their practical use in extraction. For example, weak mass transfer properties and interference of vanadium on gallium extraction contribute to hindering their application for the treatment of complex solutions such as Bayer liquor extraction [23]. There is still a need for developing new materials that could efficiently and selectively recover gallium from complex solutions with optimized mass transfer performances.

Porous silica-based sorbents are very useful supports because of the possibility to manufacture relatively small physical particle size, with high surface area and pore volume [24–30]. In many cases, especially with poorly structured materials, the sorption kinetics is limited by the resistance to intraparticle diffusion (inside the resin); decreasing the size of resin particle lead to faster kinetics. For example, D₂EHPA/SiO₂-P resin exhibited a much faster kinetics than D₂EHPA/XAD-7 resin [31]: its faster kinetics was directly correlated to their fine particle size (about 40–60 µm; this means about 10-times lower than the size of D₂EHPA/XAD-7 resin) [32].

Therefore, in this work, a composite associating silica particles and poly(acrylonitrile), is synthesized, before being functionalized with grafting of amidoxime groups, physico-chemically characterized and applied for Ga(III) sorption. Indeed, amidoxime-based resins are very efficient for metal binding [33–35]. The effect of different parameters (such as pH, temperature, presence of competitor metals) is investigated for optimizing the pH, determining the sorption isotherms and investigating the uptake kinetics. The sorption properties are

compared at pH₀ 4 (optimum value) and pH 13.7 (corresponding to alkalinity of Bayer liquor) with a conventional amidoxime-based resin (i.e., LSC-600 resin). Gallium desorption and sorbent recycling is also investigated before considering the selective recovery of gallium from complex Bayer liquor.

2. Material & methods

2.1. Material

Ga₂O₃ (purity > 99.99%) used as the main source of Ga(III), was purchased from Shanghai Macklin Biochemical Co., Ltd (Shanghai, China). The stock metal solutions were prepared at the concentration of 1000 mg L⁻¹ in 1 M sodium hydroxide solution, before being diluted with ultrapure water (UPW) to the desired concentration, just before use. In order to evaluate the impact of the composition of the solution, some experiments were also performed using Ga(NO₃)₃ salt for preparing the solutions; the Ga origin will be systematically reported in the caption of the relevant figures.

Hydroxylamine hydrochloride, divinylbenzene (DVB), acrylonitrile (AN), acetophenone, diethyl phthalate, benzoyl peroxide (BPO), ethanol, sodium hydroxide, sodium carbonate, hydrochloric acid and nitric acid were supplied by Sinopharm Chemical Reagent Co., Ltd (Shanghai, China). Commercial resin (LSC-600, Sunresin New Materials Co., Ltd., Shaanxi, China) was provided by Tiandong Aluminum Plant (Guangxi, China). Silica was supplied by Asahi Chemicals, Co Ltd. (Osaka, Japan). Table AM1 (see Additional Material Section) reports the main characteristics of silica particles and commercial resin (considered as reference material; i.e., LSC-600).

The circulating Bayer liquor, provided by China Aluminum Corporation (Beijing, China), contains 65 elements that are summarized in Table AM2 (see Additional Material Section). The most relevant elements (in terms of abundance or commercial interest) in this solution are Cs, Rb, Ga, V, Ca, and Al with concentrations as high as 230 mg L⁻¹, 380 mg L⁻¹, 182 mg L⁻¹, 96 mg L⁻¹, 98 mg L⁻¹ and 35 g L⁻¹, respectively.

2.2. Synthesis of PAO/SiO₂ resin

2.2.1. Preparation of PAN/SiO₂ resin

The composite support (SiO₂-P) with mean diameter of 50–100 µm (0.6 µm pore size, and 0.69 pore fraction) was obtained by copolymerization of styrene with divinylbenzene (SDB) and immobilized on SiO₂ particles (silica content was close to 17–18 wt%) [36,37]. One hundred g of silica particles was placed in a rotary evaporator flask and dried in vacuum for 60 min (under a pressure lower than 3000 Pa); air was then purged with a N₂ stream for 30 min. Two hundred mg of initiator (BPO) were dissolved in a mixture of 22.95 g of acrylonitrile and 3.32 mL of DVB, the reagents were then added drop wise to the mixture of diluent containing 43.66 mL of acetophenone and 29.1 mL of diethyl phthalate. The mixture was vigorously rotated for 2 h at 24 °C, before being maintained under reflux (in silicone-oil bath) at 90 °C for 7 h to complete polymerization. The produced material (silica-supported polyacrylonitrile, PAN/SiO₂) was washed several times with acetone and water to remove unreacted monomers, diluents and small molecular substances before being dried under vacuum overnight at 40 °C.

2.2.2. Functionalization of PAO/SiO₂ sorbent

A fixed amount (6.25 g) of NH₂OH-HCl was dissolved in 200 mL 1:1 (v/v) deionized water/ethanol in a three-necked flask under N₂ atmosphere, 4.58 g Na₂CO₃ were then added to the solution. Ten grams of PAN/SiO₂ sorbent were added to prepared solution under reflux at 70 °C for 5 h in a water bath [38,39]. The produced yellowish silica-based polymeric composite (silica-supported polyacrylamidoxime, PAO/SiO₂) was filtered off, washed several times with ethanol and dried in vacuum overnight at 40 °C. Figure AM1 (See Additional

Material Section) schematically shows the preparation process for composite particles of PAN/SiO₂ support and PAO/SiO₂ sorbent. Fig. 1 shows the expected structure of the synthesized resin (PAO/SiO₂).

2.3. Characterization of the sorbent

FT-IR spectrometry analysis was performed in the range 4000–400 cm⁻¹ using a Shimadzu IRTtracer-100 FT-IR spectrometer (Tokyo, Japan). All the samples were dried at 60 °C before being analyzed. Samples were conditioned as KBr disk containing 1% (w/w) finely ground material particles. Carbon, hydrogen, and nitrogen contents were determined using elemental analysis (2400 Series II CHNS/O elemental analyzer, Perkin-Elmer, Waltham, MA, USA). The thermal decompositions of PAN/SiO₂ and PAO/SiO₂ were evaluated by TG-DTA equipment (Netzsch STA 449 F3 Jupiter, NETZSCH-Gerätebau HGmbH, Selb, Germany); analysis was carried out under N₂ atmosphere conditions (in platinum cell). Morphological studies of the commercial resin and PAO/SiO₂ were performed by scanning electron microscopy (Phenom ProX SEM, Thermo Fisher Scientific, Eindhoven, The Netherlands) at an accelerating voltage of 15 kV. The chemical composition of the samples was semi-quantitatively characterized by energy dispersive X-ray analysis (integrated to Phenom ProX SEM). In addition, BET surface area and porosity of the resin were recorded with a Micromeritics TriStar II (Norcross, GA, USA) system at 77 K, and using the BET equation with N₂ gas and desorption branches of isotherms based on BJH methods, respectively. BET samples were swept for 4 h at 120 °C with N₂ gas before testing.

The pH_{PZC} was obtained using the pH-drift method [40]: 100 (\pm 5) mg of sorbent was shacked with 30 mL of a 1 M and 0.1 M NaCl at different initial pH values (pH₀ in the range 1–14); after 48 h of contact, the equilibrium pH (pH_{eq}) was determined using a S220 Seven Compact pH/Ionometer. The pH_{PZC} value corresponds to the condition: pH₀ = pH_{eq}.

XPS spectra were measured using an ESCALAB 250XI⁺ instrument (Thermo Fischer Scientific, Inc., Waltham, MA, USA) with monochromatic X-ray Al K α radiation (1486.6 eV) and the following operating parameters: spot size: 500 μ m; absolute resolved energy interval calibrated with Ag3d_{5/2} line (0.45 eV) and C1s line (0.82 eV); sample-preparation pressure was set to 10⁻⁸ mbar; the full-spectrum pass energy and the narrow-spectrum pass energy were fixed to 50 eV and 20 eV, respectively.

2.4. Sorption experiment

2.4.1. Sorption studies

Metal ion binding capacity was measured by the batch equilibration technique with varying pH solutions (pH 3 to 14) after dilution of stock metal solution (in the case of the evaluation of pH effect). To avoid precipitation at low pH values, Ga(III) solutions were dissolved in 1 (\pm 0.1) M sodium hydroxide; the concentration of Ga(III) in the solutions did not exceed 50 mg L⁻¹ (except for sorption isotherms). The presence of precipitate was systematically checked before validating experimental results. Some experiments were also performed using gallium nitrate salt for the preparation of the solutions in order to measure the relative impact of the composition of the solution (high salinity). The pH of the solutions was controlled by 0.1 M/1 M HCl or NaOH solutions.

Sorption tests were performed using a fixed solid/liquid ratio (sorbent dosage, SD) close to 280 mg L⁻¹. The suspension was maintained under agitation on a reciprocal shaker (agitation speed: 150 rpm) for 48 h. The equilibrium pH was monitored; 5 mL of the supernatant was withdrawn, filtrated on a filter membrane (0.45 μ m). The residual concentration of Ga(III) (C_{eq}, mg Ga L⁻¹ or mmol Ga L⁻¹) was analyzed by inductively coupled plasma atomic emission spectrometry (ICP-7510 Shimadzu, Tokyo, Japan) under the following conditions: 15 L min⁻¹ plasma gas flow and 0.6 L min⁻¹ nebulizer gas flow. Most of the

experiments were performed at pH close to 4. However, in order to evaluate the efficiency of the sorbents for industrial-like solutions (such as the Bayer liquor) complementary tests were also performed with solutions prepared at pH 13.7. For uptake kinetics samples were regularly contacted over 48 h of contact and filtrated samples were analyzed for residual concentration. In the case of sorption isotherms the initial concentration was varied between 20 and 300 mg Ga L⁻¹.

The sorption capacity (q, mg Ga g⁻¹ or mmol Ga g⁻¹) was calculated using the mass balance equation:

$$q = (C_0 - C_{eq})V/m \quad (1)$$

where q is sorption capacity (mg Ga g⁻¹ or mmol Ga g⁻¹), C₀ and C_{eq} are the initial and the equilibrium concentrations of gallium in solution (mg L⁻¹ or mmol L⁻¹), V and m are the volume (L) and the weight of dry sorbent (g), respectively.

Gallium desorption was tested using 1.5 M HCl solutions (SD: 400 mg L⁻¹) with a contact time set to 1 h. The recycling of the sorbent was characterized over 5 successive sorption and desorption cycles by comparing sorption and desorption efficiencies under similar experimental conditions; sorption step: the sorbent (20 mg) was mixed with a 50 mg Ga L⁻¹ solution for 24 h (SD: 400 mg L⁻¹); a rinsing step was systematically processed between each sorption and desorption step.

In order to approach the selectivity of the sorbents for Ga in complex solutions, such as the Bayer liquor, sorption capacities were determined and compared for Ga(III) (1.09 mM) in the presence of excess of Al, Mg, Ca (1.71 mM, 1.88 mM, 2.4 mM, respectively). Different pH values (in the range 1–14) were tested and the equilibrium pH values were monitored together with the determination of sorption capacities, q, and selectivity coefficient, Sc_{Me1/Me2} calculated according to:

$$Sc_{Me1/Me2} = \frac{K_d^{Me1}}{K_d^{Me2}} = \frac{\frac{q_{eq,Me1}}{C_{eq,Me1}}}{\frac{q_{eq,Me2}}{C_{eq,Me2}}} \quad (2)$$

Note: all experiments were duplicated in order to evaluate the reproducibility: the overall variation did not exceed 5%. Detailed experimental conditions are systematically reported in the caption of the figures and tables.

2.4.2. Modeling uptake kinetics and sorption isotherms

The uptake kinetics may be controlled by the intrinsic reaction rate using conventional equations (pseudo-first order reaction rate (PFOR) [41,42] and the pseudo-second order reaction rate (PSORE) [43]. These models have been initially designed for describing homogeneous chemical reaction; their extension to model heterogeneous sorption process means that the apparent rate coefficients integrate the contribution of the mechanisms of resistance to diffusion. The resistance to intraparticle diffusion was modelled using the so-called Crank equation [44]. Table AM2 (see Additional Material Section) reports the relevant equations.

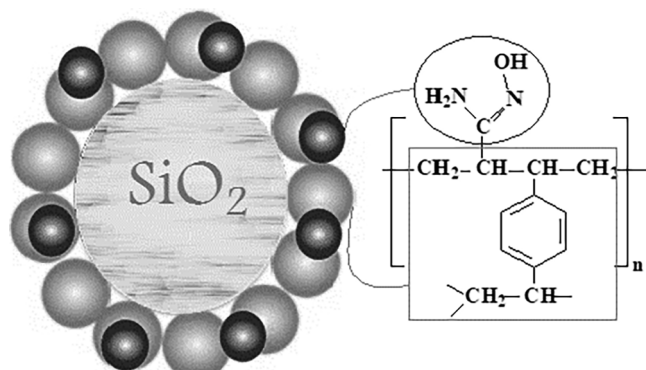


Fig. 1. Suggested structure of PAO/SiO₂ sorbent.

The sorption isotherms represent the distribution of the metal between the liquid and the solid phases at equilibrium for different initial metal concentrations. They are usually fitted by conventional models such as the equations of Langmuir [45,46], Freundlich [47] and Sips [48]. Relevant equations are reported in Table AM3 (see Additional Material Section).

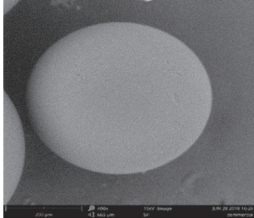
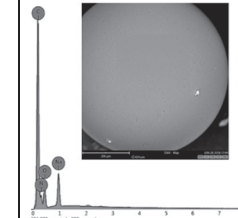
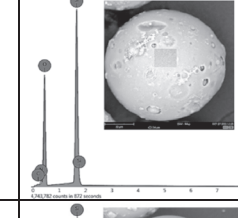
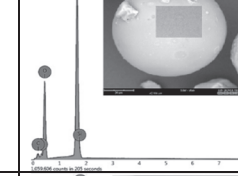
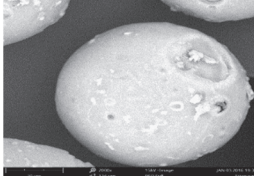
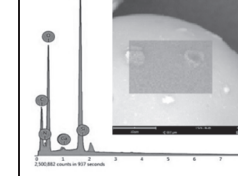
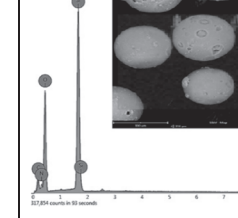
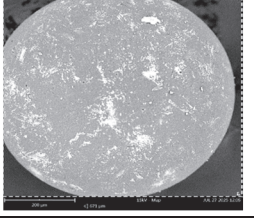
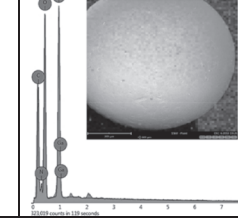
2.4.3. Tests on Bayer liquor

In order to evaluate the potential of this sorbent for industrial application, a series of tests was performed on a complex Bayer liquor sample containing 65 different elements (Table AM4, see Additional Material Section). A special attention has been paid to the selectivity of

the sorbent for Ga(III) against Al(III) and V(V) because of their large excess or their potential interest in the Bayer liquor sample. Uptake kinetics have been compared together with the distribution coefficients for Al(III) and V(V) (and then the selectivity coefficients $Sc_{Ga/V}$ and $Sc_{Ga/Al}$). The pH of the solution was adjusted at different pH values (i.e., 11.3 and 11) and the losses on precipitation of the most representative elements were determined prior to testing sorption performance on both the sorbent and the commercial resin (i.e., LSC-600). On the final step of this study, the sorbent was successfully applied toward circulating Bayer liquor with 65 metal ions, including Al(III), V(V), and Ga(III) ions.

Table 1

SEM and EDX analysis of the commercial resin, PAN/SiO₂, PAO/SiO₂ sorbent after sorption and desorption from simulated Bayer liquor.

Specification	SEM analysis	EDX analysis																								
Commercial resin		 <table border="1"> <thead> <tr> <th>Element Symbol</th> <th>Element Name</th> <th>Atomic Conc.</th> <th>Weight Conc.</th> </tr> </thead> <tbody> <tr> <td>C</td> <td>Carbon</td> <td>58.61</td> <td>52.55</td> </tr> <tr> <td>N</td> <td>Nitrogen</td> <td>22.54</td> <td>23.57</td> </tr> <tr> <td>O</td> <td>Oxygen</td> <td>16.22</td> <td>19.37</td> </tr> <tr> <td>Na</td> <td>Sodium</td> <td>2.63</td> <td>4.51</td> </tr> </tbody> </table>	Element Symbol	Element Name	Atomic Conc.	Weight Conc.	C	Carbon	58.61	52.55	N	Nitrogen	22.54	23.57	O	Oxygen	16.22	19.37	Na	Sodium	2.63	4.51				
Element Symbol	Element Name	Atomic Conc.	Weight Conc.																							
C	Carbon	58.61	52.55																							
N	Nitrogen	22.54	23.57																							
O	Oxygen	16.22	19.37																							
Na	Sodium	2.63	4.51																							
PAN/SiO ₂ sorbent		 <table border="1"> <thead> <tr> <th>Element Symbol</th> <th>Element Name</th> <th>Atomic Conc.</th> <th>Weight Conc.</th> </tr> </thead> <tbody> <tr> <td>O</td> <td>Oxygen</td> <td>45.70</td> <td>40.82</td> </tr> <tr> <td>Si</td> <td>Silicon</td> <td>25.03</td> <td>28.43</td> </tr> <tr> <td>N</td> <td>Nitrogen</td> <td>5.99</td> <td>5.86</td> </tr> <tr> <td>C</td> <td>Carbon</td> <td>23.28</td> <td>24.89</td> </tr> </tbody> </table>	Element Symbol	Element Name	Atomic Conc.	Weight Conc.	O	Oxygen	45.70	40.82	Si	Silicon	25.03	28.43	N	Nitrogen	5.99	5.86	C	Carbon	23.28	24.89				
Element Symbol	Element Name	Atomic Conc.	Weight Conc.																							
O	Oxygen	45.70	40.82																							
Si	Silicon	25.03	28.43																							
N	Nitrogen	5.99	5.86																							
C	Carbon	23.28	24.89																							
PAO/SiO ₂ sorbent		 <table border="1"> <thead> <tr> <th>Element Symbol</th> <th>Element Name</th> <th>Atomic Conc.</th> <th>Weight Conc.</th> </tr> </thead> <tbody> <tr> <td>O</td> <td>Oxygen</td> <td>50.78</td> <td>50.88</td> </tr> <tr> <td>Si</td> <td>Silicon</td> <td>16.72</td> <td>27.33</td> </tr> <tr> <td>C</td> <td>Carbon</td> <td>17.52</td> <td>10.85</td> </tr> <tr> <td>N</td> <td>Nitrogen</td> <td>14.98</td> <td>10.95</td> </tr> </tbody> </table>	Element Symbol	Element Name	Atomic Conc.	Weight Conc.	O	Oxygen	50.78	50.88	Si	Silicon	16.72	27.33	C	Carbon	17.52	10.85	N	Nitrogen	14.98	10.95				
Element Symbol	Element Name	Atomic Conc.	Weight Conc.																							
O	Oxygen	50.78	50.88																							
Si	Silicon	16.72	27.33																							
C	Carbon	17.52	10.85																							
N	Nitrogen	14.98	10.95																							
PAO/SiO ₂ sorbent + Ga(III) from simulated Bayer liquor		 <table border="1"> <thead> <tr> <th>Element Symbol</th> <th>Element Name</th> <th>Atomic Conc.</th> <th>Weight Conc.</th> </tr> </thead> <tbody> <tr> <td>O</td> <td>Oxygen</td> <td>39.54</td> <td>38.7</td> </tr> <tr> <td>Si</td> <td>Silicon</td> <td>11.14</td> <td>21.52</td> </tr> <tr> <td>C</td> <td>Carbon</td> <td>37.81</td> <td>29.22</td> </tr> <tr> <td>N</td> <td>Nitrogen</td> <td>9.97</td> <td>9.48</td> </tr> <tr> <td>Ga</td> <td>Gallium</td> <td>1.54</td> <td>1.08</td> </tr> </tbody> </table>	Element Symbol	Element Name	Atomic Conc.	Weight Conc.	O	Oxygen	39.54	38.7	Si	Silicon	11.14	21.52	C	Carbon	37.81	29.22	N	Nitrogen	9.97	9.48	Ga	Gallium	1.54	1.08
Element Symbol	Element Name	Atomic Conc.	Weight Conc.																							
O	Oxygen	39.54	38.7																							
Si	Silicon	11.14	21.52																							
C	Carbon	37.81	29.22																							
N	Nitrogen	9.97	9.48																							
Ga	Gallium	1.54	1.08																							
PAO/SiO ₂ sorbent after desorption		 <table border="1"> <thead> <tr> <th>Element Symbol</th> <th>Element Name</th> <th>Atomic Conc.</th> <th>Weight Conc.</th> </tr> </thead> <tbody> <tr> <td>O</td> <td>Oxygen</td> <td>53.67</td> <td>52.78</td> </tr> <tr> <td>C</td> <td>Carbon</td> <td>22.82</td> <td>16.85</td> </tr> <tr> <td>N</td> <td>Nitrogen</td> <td>11.81</td> <td>10.17</td> </tr> <tr> <td>Si</td> <td>Silicon</td> <td>11.70</td> <td>20.19</td> </tr> </tbody> </table>	Element Symbol	Element Name	Atomic Conc.	Weight Conc.	O	Oxygen	53.67	52.78	C	Carbon	22.82	16.85	N	Nitrogen	11.81	10.17	Si	Silicon	11.70	20.19				
Element Symbol	Element Name	Atomic Conc.	Weight Conc.																							
O	Oxygen	53.67	52.78																							
C	Carbon	22.82	16.85																							
N	Nitrogen	11.81	10.17																							
Si	Silicon	11.70	20.19																							
Commercial resin + Ga(III) from binary solution		 <table border="1"> <thead> <tr> <th>Element Symbol</th> <th>Element Name</th> <th>Atomic Conc.</th> <th>Weight Conc.</th> </tr> </thead> <tbody> <tr> <td>O</td> <td>Oxygen</td> <td>40.24</td> <td>42.78</td> </tr> <tr> <td>C</td> <td>Carbon</td> <td>38.50</td> <td>30.73</td> </tr> <tr> <td>N</td> <td>Nitrogen</td> <td>10.72</td> <td>16.47</td> </tr> <tr> <td>Na</td> <td>Sodium</td> <td>10.40</td> <td>9.68</td> </tr> <tr> <td>Ga</td> <td>Gallium</td> <td>0.07</td> <td>0.34</td> </tr> </tbody> </table>	Element Symbol	Element Name	Atomic Conc.	Weight Conc.	O	Oxygen	40.24	42.78	C	Carbon	38.50	30.73	N	Nitrogen	10.72	16.47	Na	Sodium	10.40	9.68	Ga	Gallium	0.07	0.34
Element Symbol	Element Name	Atomic Conc.	Weight Conc.																							
O	Oxygen	40.24	42.78																							
C	Carbon	38.50	30.73																							
N	Nitrogen	10.72	16.47																							
Na	Sodium	10.40	9.68																							
Ga	Gallium	0.07	0.34																							

3. Results & discussion

3.1. Characterization of the sorbent

3.1.1. Morphological investigations – SEM & SEM-EDX analysis

The morphological structure and the chemical composition of the sorbent surface have been characterized by SEM observations and EDX analysis. **Table 1** reports the characterization of commercial resin (LSC-600), PAN/SiO₂ and PAO/SiO₂ sorbents before and after sorption from highly alkaline solution (at a pH value close to those found for Bayer liquor). The SEM observation shows the difference in size of the resins: around 400–500 µm for LSC-600 commercial resin vs. 170–180 µm for PAO/SiO₂. In addition, the sorbent shows the presence of micro-pores on its rougher surface. These characteristics let expect the sorbent to get higher external and specific surface area (see below for confirmation on BET analysis).

The semi-quantitative EDX analysis confirms the high percentage of organic components (i.e., C, N, O) compared to SiO₂ support. This is a clear evidence of the successful grafting of PAN (and its amidoxime-derivative). Hence, N and O fractions increase from 5.86% and 40.82% on PAN/SiO₂ to 10.95% and 50.88% on PAO/SiO₂, respectively. The functionalization of PAN increases the density of highly reactive groups (amidoxime groups): N content increases from 4.184 mmol N g⁻¹ to 7.818 mmol N g⁻¹; this means that the substitution degree of amidoxime groups onto nitrile groups exceeds 80%.

EDX analysis was also performed on the material after being mixed with the Bayer liquor-like solution for 6 h. The mass fractions of Ga, O, N, C and Si elements reach 1.08%, 38.7%, 9.48%, 29.22% and 21.52%, respectively. The sorbent is efficient for binding Ga(III) at short contact time. The sorbent was also characterized at different contact times (up to 20 days, Table AM5, see [Additional Material Section](#)): surprisingly the EDX confirms that the amount of Ga immobilized on the sorbent decreases with contact time (above 6 h). The affinity of the sorbent for Ga(III) decreases with increasing the agitation time. In addition, the long stay of the sorbent in the alkaline Bayer liquor contributes to destabilizing the material (deformation of the spherical beads, probably associated to partial dissolving of Si in very alkaline solutions). However, Table AM5 confirms that Si content at the surface increases after being in contact with the Bayer liquor EDX analysis till 5 days of contact (up to 19.5% mass fraction) while above 5 days of contact, the Si content tends to decrease and stabilize around 15% mass fraction. The variation of Si content at the surface of the beads may be associated to Si binding and/or migration of Si from core to outer surface of the composite.

EDX analysis was also performed on Ga(III)-loaded sorbent after elution by 1.5 M HCl solution (see below). Gallium element completely disappears from the surface of the polymer: HCl is highly efficient for desorbing Ga(III) and the material is not de-structured after being in contact with highly acidic solutions. This is consistent with FTIR analysis (see below).

3.1.2. Textural properties of sorbents

The surface area, pore size, and pore volume of the commercial resin and PAO/SiO₂ are summarized in **Table 2**. The specific surface area (SSA) and pore volume of the PAO/SiO₂ resin 133.4 m² g⁻¹ and 0.7 cm³ g⁻¹ are significantly higher than the values obtained with commercial LSC-600 resin (i.e., 4.9 m² g⁻¹ and 0.1 cm³ g⁻¹ respectively). This is consistent with the strong reduction in the average pore size of the two materials: 514 Å for LSC-600 vs. 72 Å for PAN/SiO₂; it is noteworthy that the coating of silica particles strongly changes the textural properties of the support (SSA: 68 m² g⁻¹; average pore size: 686 Å). Increasing specific surface area is expected to enhance mass transfer properties and improve uptake kinetics.

3.1.3. FT-IR analysis

Fig. 2 shows the most interesting peaks of FT-IR spectra for PAN/

SiO₂ and PAO/SiO₂ materials; the spectra of Ga(III)-loaded amidoxime sorbent and metal-desorbed materials are also presented. Full scale spectra (400–4000 cm⁻¹) appear on Figure AM2 (see [Additional Material Section](#)). The peak appearing at 2240 cm⁻¹ is assigned to the stretching vibration of nitrile groups (C≡N group) on polyacrylonitrile grafted silica [49,50]; this is corroborated by the band at 2928 cm⁻¹, which is attributed to C–H stretching in aliphatic methyl groups [49]. After amidoxidation (PAO/SiO₂ sorbent), the broad band at 3422 cm⁻¹ is intensified because of the OH and NH groups (amidoxime moiety) immobilized on PAN/SiO₂ sorbent. The peak at 2240 cm⁻¹ disappears due to the grafting of amidoxime on nitrile groups [50], and a new band is appearing at 1669 cm⁻¹; this band is assigned to the stretching vibration of C=N secondary amide [51,52]: amidoxime is successfully grafted on the sorbent and replaces nitrile groups. A new peak appears at 1382 cm⁻¹ (associated to –OH stretching peak [53]). On the other hand, the peak at 939 cm⁻¹ confirms the presence of the N–O group of amidoxime [50,54]. Three peaks assigned to Si–O–Si [55] for PAN/SiO₂, PAO/SiO₂, Ga(III)-loaded sorbent and metal-desorbed material can be identified: (a) a broad peak (overlapped with C–O stretching signal) appears at 1107 cm⁻¹, 1110 cm⁻¹, 1109 cm⁻¹ and 1108 cm⁻¹, respectively [56]; (b) the peak overlapped with C–C peak appears at 800 cm⁻¹, 798 cm⁻¹, 802 cm⁻¹ and 805 cm⁻¹, respectively [55], and another one appearing at 460 cm⁻¹, 460 cm⁻¹, 463 cm⁻¹ and 464 cm⁻¹, respectively [55,57,58].

These different observations confirm the presence of the silica core, the grafting of acrylonitrile and the efficient functionalization of the nitrile groups with amidoxime moiety. The general structure of the sorbent is then confirmed.

The spectrum of Ga(III)-loaded sorbent is characterized by little shifts and decreased intensities for the peaks assigned to N–O, NH and OH peaks as shown in Fig. AM6 (see [Additional Material Section](#)). The intensities of the signals (transmittance) for –OH, C–N and –C≡N bands in PAO-SiO₂ sorbent decrease from 23%, 55% and 17% to 13%, 51% and 10%, respectively. In addition, the peak for N–O completely disappears after metal binding. This is a first indication that these chemical groups, which are characteristics of amidoxime compound, are involved in metal binding. This is consistent with the characterization of Ga(III) binding on HF528 resin (an amidoxime-modified acrylonitrile-DVB resin) [59]. Long et al. [60] reported the appearance of a peak at 595 cm⁻¹ after Ga(III) sorption on a resin bearing amidoxime groups and the weak impact of metal binding on nitrogen-based compounds: they concluded that Ga(III) sorption occurred on the O group of amidoxime group. Zhao et al. [10] also reported for Ga(III) recovery from Bayer liquor using LSC-700 amidoxime-based resin that gallate ions (i.e., Ga(OH)₄⁻) are bound on deprotonated OH group of amidoxime moiety. The large band associated to silica does not allow identifying this peak on the PAN/SiO₂ sorbent; in addition Ga(III) was bound on the sorbent at pH close to 4, where Ga(III) is not present as gallate: the sorption mechanism is probably different. It is noteworthy that after Ga(III) desorption, the spectrum of the sorbent is partially restored: the main characteristic peaks are identified again. Figure AM3 (see [Additional Material Section](#)) shows the FTIR spectra of commercial resin (LSC-600), before and after Ga(III) sorption and after metal desorption. The sorption of Ga(III) is followed by a decrease in the intensity of some peaks associated to NH and OH groups (at 3300 cm⁻¹): the functional groups C≡N–OH is involved in metal binding. This is confirmed by the weakening of the N–O peak at 970 cm⁻¹, after Ga(III) sorption. These results obtained at pH close to 4 are consistent with the

Table 2
Textural properties of PAO/SiO₂ and LSC-600 resin.

Sample name	Surface area/(m ² /g)	Pore size/Å	Pore volume/(cm ³ /g)
LSC-600	4.9	514.0	0.1
PAO/SiO ₂	133.4	72.4	0.7

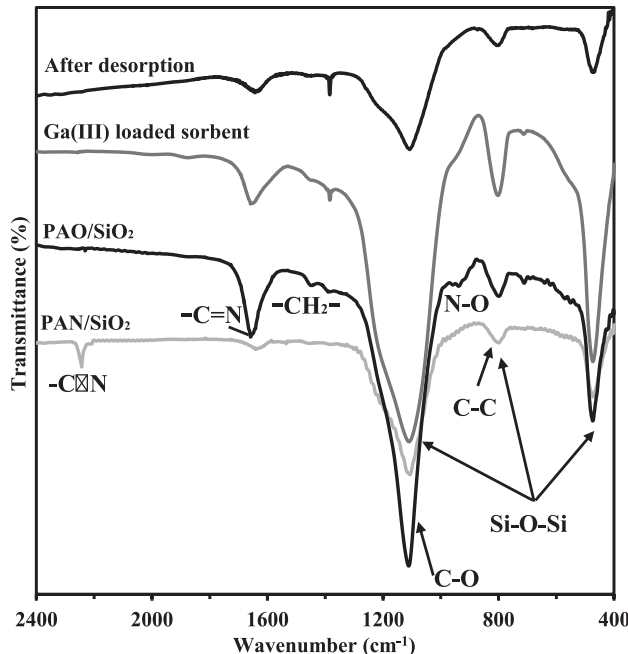


Fig. 2. FTIR spectra of PAN/SiO₂, and PAO/ SiO₂ for identifying the chemical modifications of the support; for amidoxime sorbent: spectra after Ga(III) sorption and after metal desorption (scaled to the wavenumber range: 400–2400 cm⁻¹).

observations on PAO/SiO₂ sorbent. The partial conversion of PAN into PAO (see below) also means that some nitrile groups not converted may be available for possible interactions with Ga(III) ions.

3.1.4. Element analysis

The percentages of carbon, nitrogen, and hydrogen at different stages of the synthesis procedure have been monitored by elemental analyzer. The most significant marker of the chemical modification in either PAN or PAO is the nitrogen content; this is roughly consistent with the supposed reaction pathway: nitrogen content progressively increases. As expected, the second step in the synthesis (conversion of PAN into PAO due to hydroxyl amine hydrochloride reaction) increases N content (Table 3). Nitrogen content increases from 2.94% (2.1 mmol g⁻¹) to 4.04% (2.88 mmol N g⁻¹). Based on the suggested reaction pathway (Figure AM1, see Additional Material Section) the variation in nitrogen content (close to 37%) means that the substitution degree approaches only 37%, lower than the value retained from the semi-quantitative elemental analysis obtained through EDX characterization.

3.1.5. Thermo-gravimetric analysis

The thermal stabilities of PAN and PAO resin were measured under nitrogen atmosphere using TGA (Figure AM4, see Additional Material Section). In the case of PAN sorbent, thermal decomposing is characterized by three stages: (a) first removal of water and bound solvent molecules occurs between 25.7 °C and 109.7 °C [52,61]; the mass loss counts for about 7.0%; (b) in the second stage, identified in the temperature range between 109.7 °C and 405.3 °C, the mass loss represents 19.2%; this stage is probably due to degradation of polymer backbone (with two alternative or concomitant degradations: styrene-DVB backbone and/or acrylonitrile moiety) [62]; and (c) finally, the last step (counting for about 11% in terms of weight loss) occurs between 405.3 °C and 617.9 °C (centered around 500 °C) corresponds to the final degradation of the remaining organic materials. For PAO sorbent thermal degradation, four-step mass-loss can be identified; as shown on both TGA and DSC profiles. The first mass-loss (around 9.8%) happens in the range 25.7–108.6 °C (assigned to water and solvent). The second

stage (mass-loss close to 9.7%) in the degradation process is observed between 108.6 °C and 290.5 °C; this is assigned to the decomposition of functional groups of hydroxyl and amine moieties on amidoxime backbone. It is noteworthy that this second phase in the degradation occurs at a much lower temperature than for PAN/SiO₂ material: amidoxime moiety is less thermally stable than acrylonitrile group; this is consistent with the conclusions reported by Ajmal et al. [63] and Zhari et al. [64]. The third stage in the thermal degradation of PAO/ SiO₂ ranges between 290.5 °C and 407 °C (about 18.6% mass-loss); this is assigned to the decomposition of the polymer chain. The final stage takes place between 407 °C and 690 °C (counting for 9.9 mass-loss); this is attributed to the final degradation of the remaining organic materials [65]. The total mass losses represent 36.7% and 48.0% for PAN/SiO₂ and PAO/SiO₂ sorbents, respectively. This clearly demonstrates the increase in hydrocarbon content in the amidoximated material compared to its PAN precursor. On the other hand, the residual material at temperature above 700 °C represents the approximate amount of silica core in the resins (i.e., about 63% and 52% for PAN/SiO₂ and PAO/SiO₂ sorbents, respectively); a substantial part of the materials is represented by inactive silica core.

3.1.6. pH_{PZC} analysis

Fig. 3 shows the titration curve for the determination of the pH_{PZC} (pH-drift method); two experiments were performed changing the concentration of the background salt (i.e., 1 M and 0.1 M NaCl). The maximum pH variation is reached at pH₀ around 4 (i.e., ΔpH between 1.5 and 2.4, depending on the background salt). The values of pH_{PZC} are very close (i.e., 6.84 and 6.85 for 1 M and 0.1 M NaCl, respectively). This means that the PAO/SiO₂ sorbent is positively charged in acidic solutions and negatively charged in alkaline solutions. The positively charged sorbent may repulse cationic species; increasing the pH decreases the positive charge of the material and then reduces the repulsive effects. These characteristics will be critical for pH control on sorption performance through the attraction/repulsion effects crossed to the effects of metal speciation.

3.1.7. XPS identification

XPS analysis was performed on the sorbent before and after Ga(III) sorption in order to confirm the sorption mechanism (Fig. 4: full XPS survey). Table AM7 (see Additional Material Section) shows the XPS spectra of the C 1s, O 1s, N 1s and Ga 2p signals (including band deconvolution) while Table AM8 (see Additional Material Section) reports the assignment of the deconvoluted bands and their relative atomic fractions. The effective sorption of Ga(III) is confirmed by the appearance of the specific Ga 3d signals but also by substantial shifts in the binding energies (BEs) of selected signals and appearance of new peaks (in the deconvoluted profiles) because of the modification of their chemical environment after metal binding. In the 1110–1150 eV range, two peaks are appearing (corresponding to Ga 2p_{3/2} and Ga 2p_{1/2} bands, around 1117.6 eV [66] and 1144.3 eV, respectively; the splitting spin-orbit is close to 27 eV) and a loss feature for a BE of 1132 eV. The individual bands can be deconvoluted with a large peak corresponding to Ga(III) bound species and a much smaller peak corresponding to native oxide at higher BEs (i.e., close to 1119.6 eV and 1144.7 eV).

For C 1s bands, the deconvolution of the signal into bands associated with C–C, C–H, C–NH₂ and C=NOH contributions and the comparison of XPS spectra for raw material and metal-loaded sorbent show a

Table 3

Chemical compositions (C, H and N mass percentages) of PAN/SiO₂ and PAO/ SiO₂.

Sample name	C (%)	H (%)	N (%)	N (mmol. g ⁻¹)
PAN/SiO ₂	12.52	1.323	2.94	2.10
PAO/SiO ₂	12.55	1.644	4.04	2.88

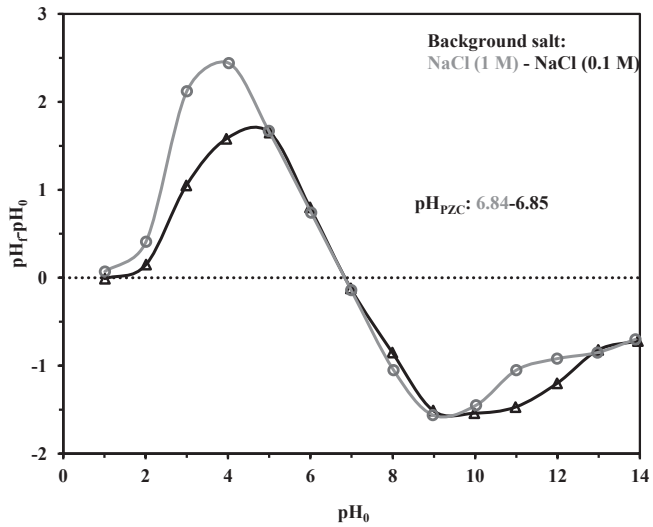


Fig. 3. Determination of pH_{PZC} by the pH-drift method (sorbent dosage, SD: 2 g L^{-1} ; background salt: (1 M NaCl (grey symbols), and 0.1 M NaCl (black symbols)); contact time: 48 h).

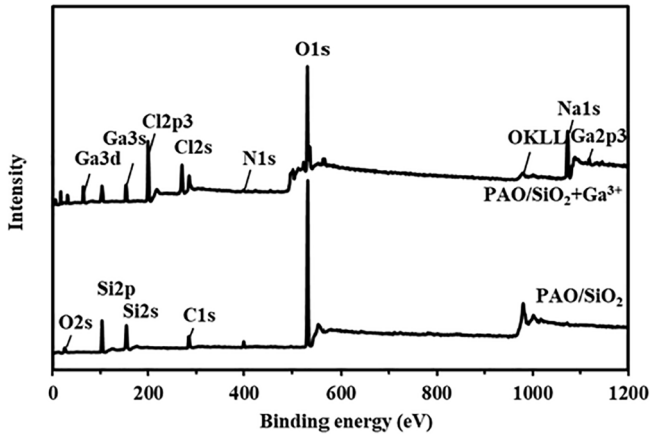


Fig. 4. XPS spectra of PAO/SiO₂ before and after Ga(III) loading (full survey).

shift of the BEs of the nitrogen-based groups (i.e., C–NH₂ and C=NOH) toward higher BEs ($+ \approx 2 \text{ eV}$). This clearly demonstrates that the environment of C element in these reactive groups has been affected by gallium binding.

Table AM8 (see Additional Material Section) reports very small shifts for C–O and O–H signals on O 1s signal [67]. These reactive groups (on amidoxime moiety) are shifted by 0.3–0.4 eV. The O 1s signal (at 532.48 eV), assigned to SiO₂ [68,69], is not affected by metal binding. A new peak, assigned to O–Ga, is also appearing at 530.3 eV; this may be attributed to either Ga precipitate or interaction of amidoxime with Ga(III).

The comparison of the signal N 1s on the sorbent before and after Ga(III) sorption shows poor variation in the band corresponding to –NH₂ in terms of BE while its relative atomic fraction decreases by about 25%. On the opposite hand, the deconvoluted band that corresponds to =NOH is increased in terms of atomic fraction while its BE is shifted toward lower BE after Ga(III) sorption. In addition, a new signal at 398.35 eV, assigned to N–Ga clearly confirms the interaction of amidoxime moiety with Ga(III).

XPS spectra demonstrate that both O- and N- based reactive groups of amidoxime moieties are sharing electrons with Ga(III) after metal binding.

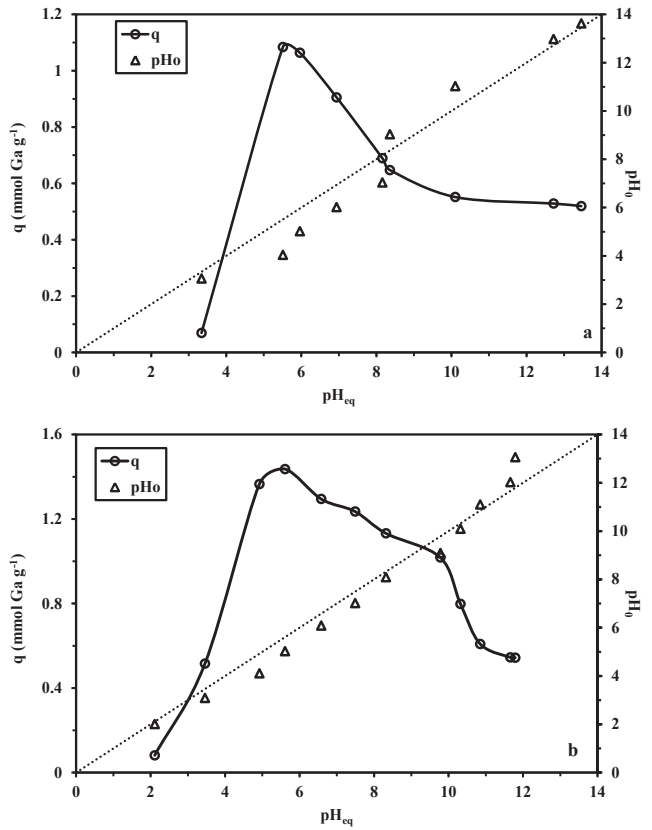


Fig. 5. Effect of pH on sorption capacity for Ga(III) using PAN/SiO₂ and pH variation during metal sorption: (a) Ga₂O₃ solution, (b) Ga(NO₃)₃ solution (Sorbent dosage, SD: 280 mg L^{-1} ; C_0 : 0.567 mmol Ga L⁻¹; T: 25°C ; agitation speed: 150 rpm; contact time: 48 h).

3.2. Sorption properties

3.2.1. pH effect

The pH is a critical parameter in the management of sorption processes, especially for the binding of metal ions. Indeed, the pH influences the speciation of the metal in solution (hydrolysis, complexation, precipitation [70,71]) and the ionic charge of reactive groups at the surface of the sorbent (protonation and deprotonation of functional groups).

Fig. 5 shows that the pH is hardly affected during metal sorption: the variation does not exceed 0.8 pH unit. The sorption capacity is sharply increased between pH 2 and 4, reaches a maximum around 5.2 and progressively decreases with increasing the pH. This can be directly correlated with the predominating Ga(III) species. In acidic solutions, free Ga(III) is predominating: below pH 3, Ga³⁺ is the major species and Ga(OH)²⁺ fraction progressively increases with pH. Between pH 3 and 4.5, protonated hydrolyzed species predominate (Ga(OH)²⁺ and Ga(OH)₂⁺ to a lesser extent). Anionic hydrolyzed species (i.e., Ga(OH)₄⁻) begins to form at pH 3.8 and becomes predominant at pH higher than 4.5 (at this pH, neutral species Ga(OH)₃ reaches its maximum fraction close to 10% of total gallium) [71]. Zhang et al. [70] report slightly different predominance ranges around pH 5: between pH 4 and 6, they report predominance of the neutral species (i.e., Ga(OH)₃) while the anionic species (i.e., Ga(OH)₄⁻) becomes to form at pH 4 and predominates over pH 6. The pH_{PZC} of the sorbent has been determined by the pH-drift method (see above, Section 3.1.6.) close to 6.85. At pH below 6.85, the sorbent is protonated and positively charged: this may repulse metal cations and explain the low sorption capacity of PAO/SiO₂ sorbent; with the pH increase the sorption repulsion progressively decreases and enhances metal binding. A pH close to 5–5.5 seems to be

a good compromise between metal speciation and protonation/deprotonation properties of the reactive groups of the sorbent. Amidoxime moieties have been characterized as the main functional groups involved in metal binding (FTIR and XPS characterizations). Zhao et al. [10] discussed the mechanisms involved in Ga(III) binding using amidoxime-based sorbent. They reported that 3 different mechanisms can explain metal ion sorption on amidoxime groups: (a) binding on oxygen group (from $-\text{OH}$), (b) binding on both O and N donor atoms (to form a 5-membered chelate ring), and (c) the third mode that involves η^2 interaction with N–O oximido reactive group. Based on FTIR analysis they concluded that Ga(III) was bound by deprotonation of $-\text{OH}$ group and local binding. In the present case, FTIR and XPS analyses have shown that the chemical environment of N and O reactive groups have been affected by Ga(III) sorption. The chelate formation appears to be more appropriate for describing metal binding; similar mechanism was reported for the binding of uranium on amidoxime-based sorbent [72]. This is consistent with the deprotonation of $-\text{OH}$ and NH groups. The decrease of sorption capacity with increasing pH is associated to the change in protonation of the sorbent, and the shielding effect of Na^+ ions on N and O reactive groups.

The profiles shown on Fig. 5 for solutions prepared by Ga_2O_3 mineralization in NaOH solutions and by dissolving of $\text{Ga}(\text{NO}_3)_3$ salt do not differ in the pH edges and the maximum sorption is equally observed around pH 5. The main difference is reported in terms of sorption capacities: the nitrate salt allows reaching a higher sorption capacity under comparable experimental conditions (i.e., $1.44 \text{ mmol Ga g}^{-1}$ vs. $1.08 \text{ mmol Ga g}^{-1}$). The high ionic strength associated to NaOH dissolving contributes to decrease the availability of reactive groups (due to competition or shielding effects).

The occurrence of metal hydrolysis and precipitation phenomena at high concentration at pH 5–5.5 make selecting pH 4 as the working pH more appropriate for further basic studies. However, the sorption studies were also performed at pH 13.7 for evaluating sorption performance for industrial effluents like Bayer liquor. In highly alkaline solutions, Ga(III) is present as hydrolyzed anionic species (i.e., mainly Ga(OH)_5^{2-}) [70,71].

3.2.2. Uptake kinetics

The uptake kinetics has been investigated at pH 4 and pH 13.7 for both PAO/SiO₂ and LSC-600 (a commercial amidoxime-based resin) (Figs. 6–8). The analysis of kinetic profiles does not bring only information on the time required for reaching equilibrium but also on the stability of the material (and its interaction with target solute) and on the controlling step in the sorption mechanism.

Under selected experimental conditions (i.e., SD: 0.25 mg L^{-1} and gallium concentration in the range $20\text{--}40 \text{ mg G a L}^{-1}$ or $0.364\text{--}0.595 \text{ mmol Ga L}^{-1}$) at pH 4.01, the time required for reaching the equilibrium does not exceed 60 min (Figs. 6 and 7). Seventy % of total sorption occurs within the first 15 min of contact: sorption takes place on the very accessible sorption sites at the surface of the sorbent and the first external layers of the material. In the second step, a slower sorption occurs driven by the diffusion into the pores of the composite sorbent (amidoximated PAN immobilized on silica particles). Fig. 6 compares the modeling of kinetic profiles with the 3 models (i.e., PFORE, PSORE and RIDE) for PAO/SiO₂ and the commercial amidoxime resin (LSC-600). The sorption kinetics are comparable: the contact time required for reaching equilibrium (about 60 min) is of the same order of magnitude for the two sorbents; although the equilibrium concentration is significantly lower for PAO/SiO₂. Table 4 reports the parameters of the models for the two sorbents. For solutions prepared by mineralization of Ga_2O_3 in NaOH the kinetic profiles were best fitted by the PSORE and the RIDE equations, while for the solution prepared with $\text{Ga}(\text{NO}_3)_3$ salt the PFORE and the RIDE fits better experimental profiles (lower estimated variance, EV and calculated sorption capacity at equilibrium closer to experimental value of $q_{\text{eq},\text{exp}}$). These data also shows that the rate coefficients and the equilibrium sorption capacities

are higher for PAO/SiO₂ than for LSC-600 resin. The intraparticle diffusivity of Ga(III) in the sorbents depends on the composition of the solution but remains in the range $0.59\text{--}1.10 \times 10^{-10} \text{ m}^2 \text{ min}^{-1}$ for PAO/SiO₂ and around $1.6 \times 10^{-10} \text{ m}^2 \text{ min}^{-1}$ for LSC-600. The slightly higher diffusivity of Ga(III) in the commercial resin can be explained by the larger size of pores (Table 2); however, this effect is reduced by the much higher specific surface area of the PAO/SiO₂ sorbent. The composite sorbent appears competitive under selected experimental conditions with the commercial resin.

At pH 13.7, the sorption of Ga(III) is poorly efficient with LSC-600 resin: under selected experimental conditions (C_0 : 90 mg Ga L^{-1} or $1.326 \text{ mmol Ga L}^{-1}$, and SD: 0.3 g L^{-1}) the sorption capacity remains below 4 mg Ga g^{-1} (Fig. 8). The PAO/SiO₂ resin shows a very complex kinetic profiles that can be decomposed in three phases: (a) strong decrease in relative Ga(III) concentration within the first 30 min of contact, (b) stabilization of sorption (constant residual Ga(III)

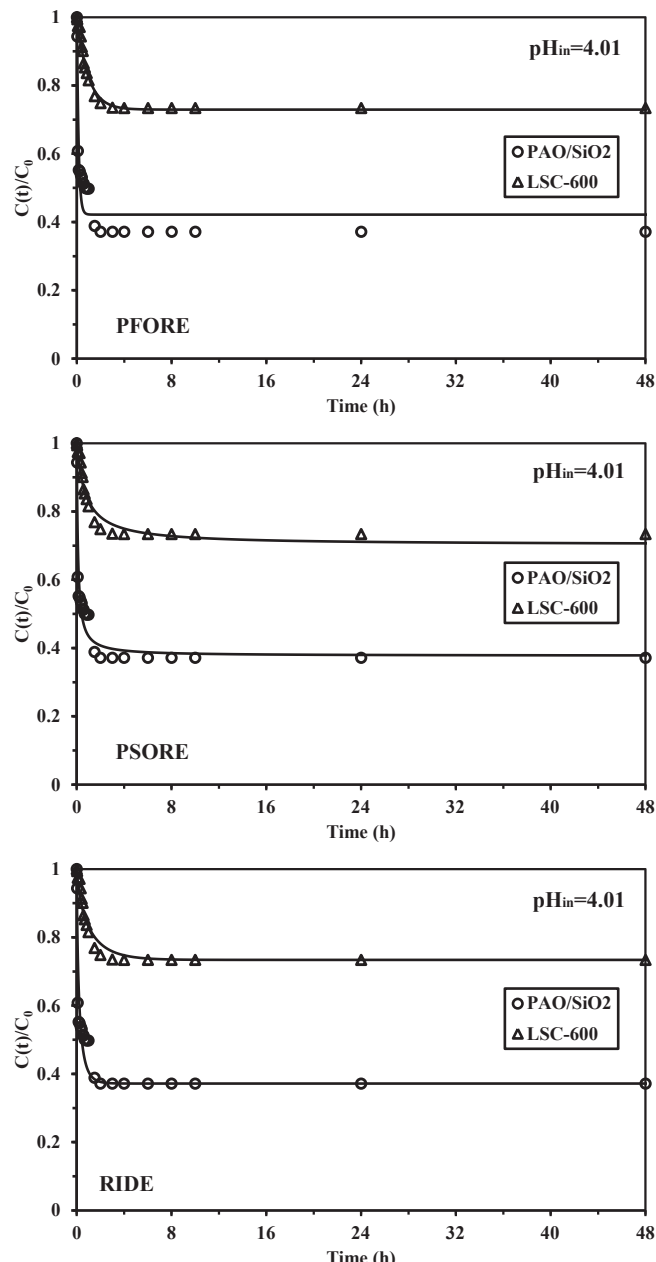


Fig. 6. Comparison of kinetic profiles for Ga(III) sorption using PAO/SiO₂ sorbent and LSC-600 commercial resin (C_0 : 25 mg Ga L^{-1} – $0.364 \text{ mmol Ga L}^{-1}$; SD: 0.25 g L^{-1} ; pH₀: 4.12; T: 25°C ; Ga_2O_3 dissolved in NaOH solution).

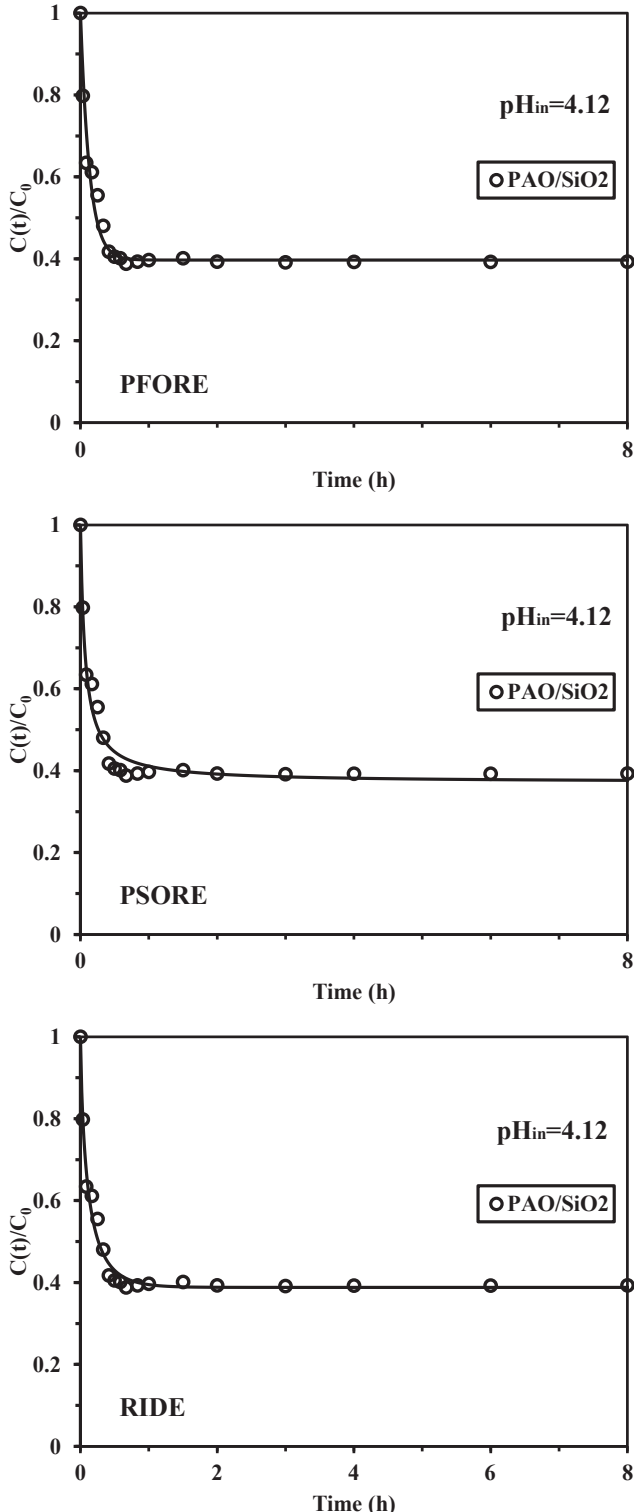


Fig. 7. Modeling of Ga(III) uptake kinetics on PAO/SiO₂ using the PFORE and RIDE equations (C_0 : 40 mg Ga L⁻¹ – 0.595 mmol Ga L⁻¹; SD: 0.25 g L⁻¹; pH₀: 4.12; T: 25 °C; Ga(NO₃)₃ salt).

concentration between 15 and 30 min and 90 min of contact (with a sorption capacity close to 35 mg Ga g⁻¹), and (c) progressive release of bound Ga(III) (after 48 h of contact the sorption capacity is below 1 mg Ga g⁻¹). The disappearance of Ga(III) is confirmed by the SEM-EDX semi-quantitative analysis of PAO/SiO₂ exposed to Bayer liquor for increasing contact time (Table AM4, see Additional Material Section).

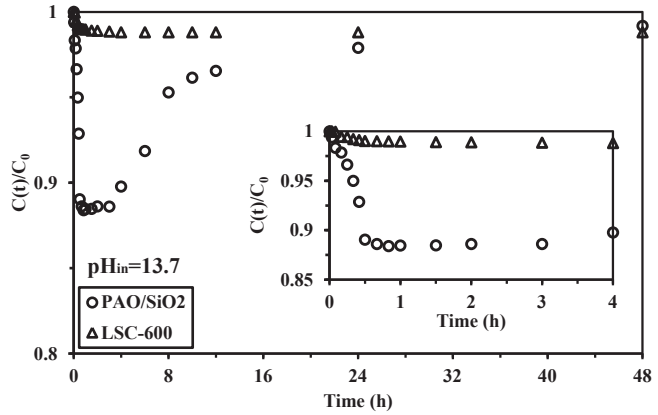


Fig. 8. Comparison of kinetic profiles for Ga(III) sorption using PAO/SiO₂ sorbent and LSC-600 commercial resin (C_0 : 90 mg Ga L⁻¹ – 1.326 mmol Ga L⁻¹; SD: 0.3 g L⁻¹; pH₀: 13.7; pH_{eq}: 12.13; T: 25 °C).

The surface of resin particles is progressively damaged and the analysis of surface shows the presence of increasing amounts of Na element and important fluctuations in the weight percentages of elements such as C or Si. The aggressive conditions of Bayer liquor cause partial degradation of the support and competition or screening effects of ions present in high concentration (such as sodium). This may explain this progressive loss of sorption performance. While using PAO/SiO₂ sorbent for the treatment of Bayer liquor it will be necessary limiting the contact of the resin with the solution below 90 min using batch mode preferentially to fixed-bed column system.

Other sorbents used for the recovery of gallium from aqueous solutions were characterized by similar or even higher equilibrium time than PAO/SiO₂: IRA-910, ES-346 and PAO-AN-DVB required equilibrium times as high as 150, 240 and 40 min, respectively [11,73,74].

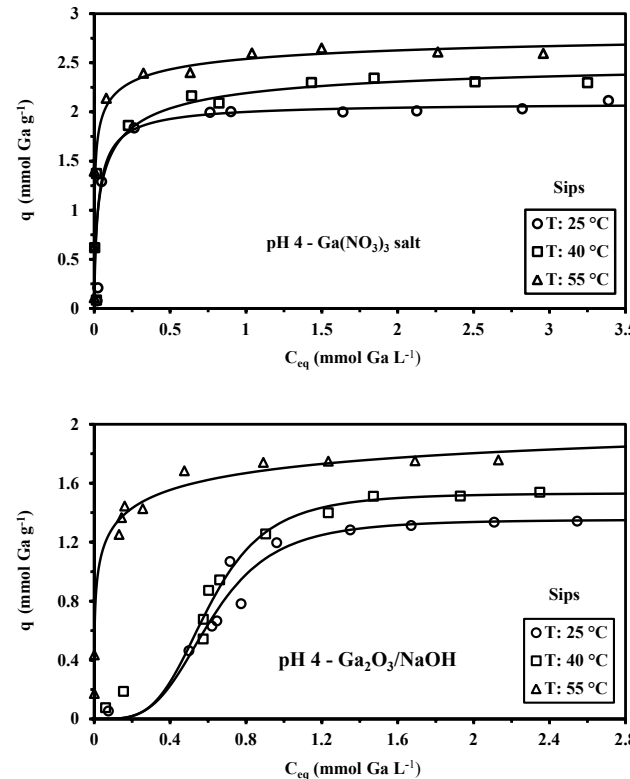
3.2.3. Sorption isotherms

The Ga(III) sorption isotherms were carried out at pH 4 with PAO/SiO₂ sorbent at 3 temperatures (i.e., 25, 40 and 55 °C) in two kind of matrices (Ga(NO₃)₃ and Ga₂O₃ mineralized in NaOH solution) (Fig. 9). The nitrate-based solution shows the conventional profile typical of Langmuir-type isotherm whatever the temperature: (a) strong increase of sorption capacity, followed by (b) a saturation plateau. The maximum sorption capacity increases with temperature: the sorption mechanism is endothermic. For Ga(III) sorption isotherm at pH 4 in the case of complex solutions (prepared by Ga₂O₃ dissolving in NaOH) the profiles are atypical at T: 25 °C and 40 °C. The sorption isotherm are characterized by a sigmoidal trend: the profile begins with an unfavorable trend with the sorption that remains negligible below a limit Ga(III) concentration (close to 0.2 mmol Ga L⁻¹) before strongly increasing. The high salinity (presence of sodium) may introduce at low metal concentration an important competition between the sorbent and Na(I) for binding/complexing gallate ions. At T: 55 °C, this effect is not noticeable: the profile is close to the Langmuir-type shape. For the sorption isotherms obtained at pH 13.7 with Ga₂O₃/NaOH solutions (Fig. 9) the same trends are observed: conventional Langmuir-type profile at T: 55 °C, sigmoidal shape at T: 25 °C and T: 40 °C.

The modeling of sorption isotherms by conventional Langmuir and Freundlich models is made difficult by the sigmoidal shape of the curves. Actually, the Sips model allows fitting much better the curvatures of the isotherms (Figs. 8 and 9). Table 5 shows the parameters of the models at the different temperature and for the different types of solutions. The power-type form of the Freundlich equation is not appropriate to fit the saturation plateaus. The Langmuir equation gives good fit of isotherms in the case of gallium nitrate solutions and for gallium-complex solutions at T: 55 °C. In most cases, the Sips equation gives much better mathematic correlation; obviously the introduction

Table 4Kinetic parameters for the sorption of Ga(III) at pH 4 using PAO/SiO₂ and LSC-600.

Sorbent	C ₀ (mg Ga L ⁻¹) [mmol Ga L ⁻¹]	q _{eq,exp} (mmol Ga g ⁻¹)	PFORE		PSORE			RIDE	
			q _{eq,1} (mmol Ga g ⁻¹)	k ₁ × 10 ² (min ⁻¹)	EV	q _{eq,2} (mmol Ga g ⁻¹)	k ₂ × 10 ² (L mmol ⁻¹ min ⁻¹)	EV	D _e × 10 ¹⁰ (m ² min ⁻¹)
PAO/SiO ₂ [*]	40 [0.595]	1.44	1.42	12.7	0.0058	1.48	16.6	0.0044	1.10
PAO/SiO ₂ ^{**}	25 [0.364]	0.908	0.836	11.5	0.0094	0.900	18.0	0.0046	0.59
LSC-600 ^{**}	25 [0.364]	0.384	0.391	1.76	0.00035	0.431	5.07	0.00108	1.61

(Experimental conditions - SD: 0.25 g L⁻¹; pH₀: 4.12; T: 25 °C; *: Ga(NO₃)₃ solution; **: Ga₂O₃/NaOH solution).**Fig. 9.** Ga(III) sorption isotherms at different temperatures using PAO/SiO₂ sorbent at pH 4 using Ga(III) solutions prepared by dissolving of Ga₂O₃ in NaOH solution or Ga(NO₃)₃ salt.

of a third-adjustable parameter facilitates the mathematical fit. However, the simulated curves show a better approximation of the inflection at low metal concentration than the Langmuir equation (see Fig. 10).

Apart the thermodynamic effect, increasing the temperature may

contribute to increase pore size of the sorbent via the expansion of the polymer network; this make ions passing through the pores more freely [75]. With temperature increase, the swelling of the polymeric matrix and the additional energy brought to the system contribute to overcome the mass resistance to ion transfer [76,77].

The comparison of maximum sorption capacities for PAO/SiO₂ under different experimental conditions (temperature, pH and composition of the solution) shows great differences. Under the most favorable conditions (i.e., gallium nitrate solutions, at pH 4) the maximum sorption capacity varies between 2.12 and 2.61 mmol Ga g⁻¹. This value is consistent with the nitrogen content in the sorbent (i.e., 2.88 mmol N g⁻¹) (Table 2). This means that Ga(III) can be bound to the sorbent through interactions with both -NH₂ and -NHOH reactive groups. In the case of less favorable conditions (i.e., pH 4 with complex solutions and high salinity due to Ga₂O₃ dissolving in NaOH) the maximum sorption capacities range between 1.34 and 1.76 mmol Ga g⁻¹. In this case the molar ratio between Ga(III) and -N groups is closer to 1:1; this means that the metal ion is probably bound on either -NH₂ or -NHOH groups due to the competition of ions and the effect of ionic strength. The molar ratio between Ga(III) and N is even worst in the case of the sorption of Ga(III) at pH 13.7 from complex solution (Bayer liquor-like pH): maximum sorption capacities range between 0.52 and 0.80 mmol Ga g⁻¹. The change in pH affects metal speciation, and sorption mechanism; in addition, the ionic strength limits the availability of reactive groups for metal binding.

In order to standardize the conditions for calculation of thermodynamic parameters, the Sips equation was used for calculating the sorption capacity of the sorbent under the different experimental conditions for a standard equilibrium concentration of 1 mmol Ga L⁻¹. The values were used for calculating the distribution coefficients K_d = q_{eq} / C_{eq} (mL g⁻¹). The Van't Hoff equation was used for calculating thermodynamic parameters (change in system entropy: ΔS⁰, enthalpy: ΔH⁰ and free energy: ΔG⁰)

$$\ln K_d = \frac{\Delta S^0}{R} - \frac{\Delta H^0}{RT} \quad (1a)$$

$$\Delta G^0 = \Delta H^0 - T\Delta S^0 \quad (1b)$$

Table 5Ga(III) sorption isotherms using PAO/SiO₂ sorbent at pH 4 and different temperatures – Modeling with the Langmuir, Freundlich and Sips equations.

Salt background	T (°C)	pH	q _{m,exp} (mmol Ga g ⁻¹)	Langmuir		Freundlich			Sips			
				q _{m,L} (mmol Ga g ⁻¹)	b (L mmol ⁻¹)	R ²	k _F	n	R ²	q _{m,S} (mmol Ga g ⁻¹)	b _S (L mmol ⁻¹)	n _S
Ga ₂ O ₃ /NaOH	25	4	1.34	2.10	0.909	0.887	1.954	0.950	0.832	1.354	6.01	0.269
	40	4	1.54	2.60	0.772	0.939	1.728	1.074	0.899	1.533	7.10	0.256
	55	4	1.76	1.82	19.7	0.944	6.599	1.714	0.944	2.343	2.66	3.04
Ga(NO ₃) ₃	25	4	2.12	2.14	14.4	0.928	4.448	1.777	0.746	2.102	20.0	1.20
	40	4	2.31	2.28	34.9	0.828	5.338	2.060	0.793	2.583	5.60	1.70
	55	4	2.61	2.49	542	0.825	7.408	2.480	0.830	2.956	6.10	2.58
Ga ₂ O ₃ /NaOH	25	13.7	0.52	0.688	1.327	0.691	2.207	0.354	0.631	0.537	4.03	0.501
	40	13.7	0.61	0.838	1.094	0.860	2.049	0.400	0.796	0.682	2.05	0.677
	55	13.7	0.80	0.994	1.576	0.981	2.415	0.561	0.950	1.005	1.52	1.020

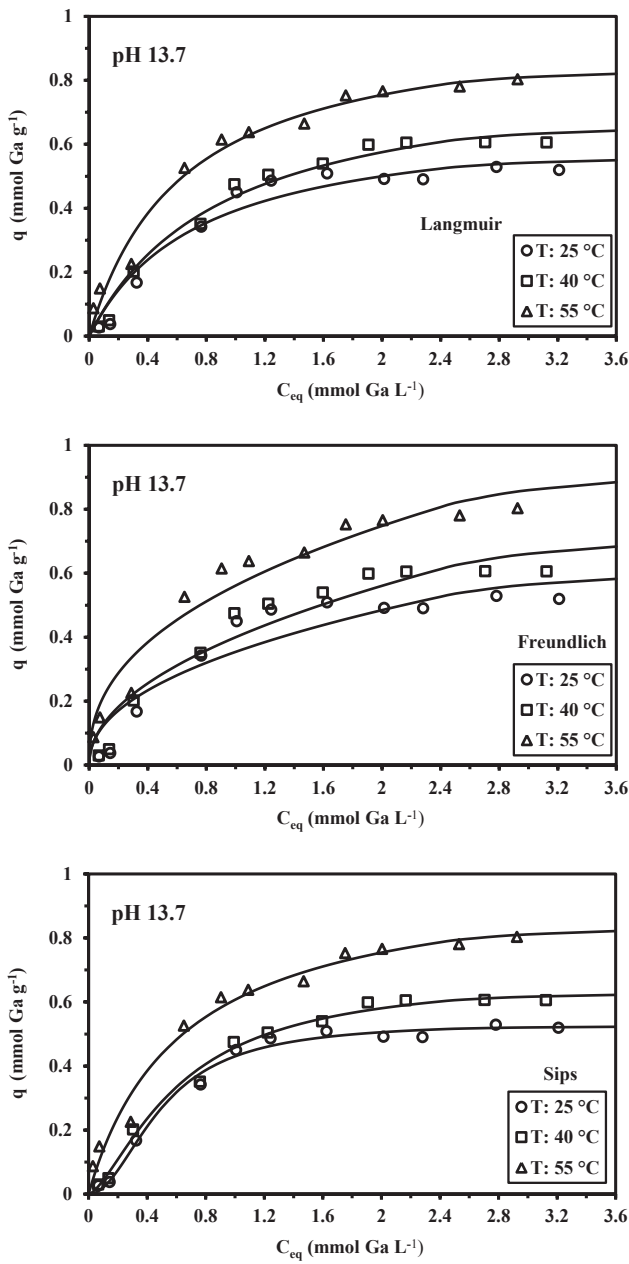


Fig. 10. Ga(III) sorption isotherms at different temperatures using PAO/SiO₂ sorbent at pH 13.7 – Comparison of isotherm models (solutions prepared by dissolving Ga₂O₃ in NaOH solution).

Table AM9 (see [Additional Material Section](#)) reports the thermodynamic parameters for the sorption of Ga(III) on PAO/SiO₂ under different experimental conditions. The negative values of ΔG^0 and the positive values of ΔH^0 mean that the sorption of Ga(III) is spontaneous and endothermic. On the other hand, the positive value of the entropy indicates that the randomness of the system increases with the sorption of Ga(III) at the interface solution/sorbent.

The sorption capacities of PAO/SiO₂ for Ga(III) are compared in [Table 6](#) to the sorption capacities of alternative materials (biosorbents, sorbents, resins, impregnated resins, minerals or activated carbon) for synthetic or Bayer Liquor solutions. As a general comment, the sorption properties of grafted composite are: (a) higher than biosorbents, and some amidoxime resins; (b) comparable to those obtained with several resins like CL-P204 Levextrel resin, but (c) lower than some of the most efficient Ga(III) sorbents like P507 extraction resin

and 3-IDA-EPI-OCS.

3.2.4. Metal desorption and sorbent recycling

Metal desorption is a key step in the design of sorption process since the competitiveness of the process is controlled by the necessity to recycle the sorbent. In addition, the desorption step, if well optimized, allows substantially increasing the concentration of the target metal in the eluate. This can be also the opportunity to contribute to the separation of the target metal from competitor metals (which could be co-adsorbed during the sorption step).

The sorbent collected after kinetic tests on pH 4 solution has been used for evaluating the desorption kinetics (Figure AM7, see [Additional Material Section](#)). An acidic solution (1.5 M HCl solution) has been selected for processing metal elution. The acid is expected to displace the equilibrium due to the protonation of reactive groups (consistently with the effect of pH on Ga(III) sorption). A contact time of 30 min is sufficient for desorbing about 96% of gallium bound to PAO-SiO₂, while the complete desorption is achieved within 40 min of agitation (at the agitation speed of 150 rpm).

The recycling was tested over five successive cycles of sorption/desorption, using again 1.5 M HCl solutions for metal elution and a water rinsing step between each sorption and desorption steps. [Fig. 11](#) compares the efficiencies of sorption and desorption at each cycle. The sorption and desorption performances remain remarkably stable (losses in efficiency remain below 10% and 8%, respectively).

The stability of the sorbent at the end of the 5 sorption/desorption cycles was monitored by SEM-EDX analysis (Figure AM 8, see [Additional Material Section](#)). The general structure of sorbent is not affected despite the use of 1.5 M HCl solution. The semi-quantitative analysis does not show drastic changes in the chemical composition of the sorbent; this is consistent with the FTIR analysis of the sorbent (see [Section 3.1.3](#)). The reactive groups are not significantly affected by the alternating steps of sorption and desorption.

3.2.5. Sorption in multi-metal solutions – Selectivity properties

The complexity of industrial effluents, of ore leachates may strongly influence (and decrease) sorption properties. It is thus necessary before evaluating the feasibility of the global process to evaluate the impact of complex matrices on sorption performance. In order to reach a better overview of the ability of PAO/SiO₂ for treating Bayer liquor a first step consisted in testing the sorption of Ga(III) in a multi-metal solution containing Mg(II), Al(III) and Ca(II) (in excess compared to Ga(III)).

Table 6

Comparison of Ga(III) sorption capacities (mg g⁻¹) for different types of sorbents.

Sorbent	pH	q (mg Ga g ⁻¹)	References
Crab shell, chitosan (powder)	2.4	17.0	[78]
		10.6	
CL-P204 Levextrel resin	2.8	42.5	[79]
P507 extraction resin	3.0	82.3	[80]
Discarded tea	3	5.6	[81]
Ga(III)-imprinted/CNTs	3.0	5.2	[82]
Bentonite	2.5	10.7	[83]
Nano-TiO ₂	7.3	4.1	[84]
3-IDA-EPI-OCS	2.8	139.6	[70]
Amidoxime resin	–	29.2	[10]
Hydroxamic Acid Resin	–	8.6	[53]
Activated charcoal	–	5.8	[85]
PAO/SiO ₂	4.01	63.3	This work
D201	14	0.19	This work
IRA900	14	0.11	This work
LSC-600 resin	13.7	3.6	This work
LSC-600 resin	4.01	26.7	This work
SiO ₂	14	0.00	This work
PAN/SiO ₂	14	0.01	This work
PAO/SiO ₂	13.7	35.2	This work

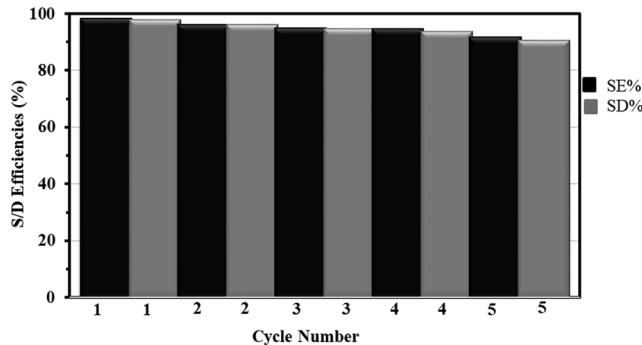


Fig. 11. Sorbent recycling at different volumetric ratios between the sorption step and the desorption step ($V_{\text{sorpt}}/V_{\text{des}}$) (Sorption step: C_0 : 50 mg Ga L⁻¹; pH 4; SD: 1 g L⁻¹; contact time: 24 h – Desorption step: 1.5 M HCl solution; contact time: 2 h; SD: 0.9 g L⁻¹; T: 25 °C).

This test was carried at different pH values (pH_0 in the range 1–13) in order to select the most appropriate conditions for selective separation.

Fig. 12 shows the strong impact of pH on the selectivity coefficients Ga(III)/Mg(II), Ga(III)/Al(III) and Ga(III)/Ca(II). Sorption levels for metal cations are very low at pH 1.22 and the selectivity is negligible. On the other side, at higher pHs, the sorbent has a strong selectivity against cations, especially against Mg(II): the selectivity coefficient SC(Ga/Mg) is maximum (around 450–500) for pH in the range 4–6; at higher pH the selectivity decreases and stabilizes around 100 at pH higher than 7.5 (selectivity below 50 for pH lower than 4). The optimal selectivity against Ca(II) is slightly shifted toward pH 5.5–7.2 (with SC(Ga/Ca) close to 220–320); the SC stabilizes around 100 in a large range of pH values (2.28–4.18 and 7.38–8.71) but increases again in very alkaline solutions to reach a value as high as 430 at pH 12.8. For Al(III) the highest selectivity coefficients are obtained at pH 2.28–3.27 (SC(Ga/Al) around 180) and at pH higher than 7.8 (SC(Ga/Al) varying between 250 and 340). The lowest SC are generally obtained around pH 7.5, probably because of indistinct precipitation phenomena.

In any case the sorbent has a remarkable preference for Ga(III) over selected metal cations making possible the separation of Ga(III) from multi-metal solutions; taking into account the beneficial effect of optimizing pH choice. Figure AM9 (see Additional Material Section) schematizes the preferential pH ranges for optimizing separation. The molar fraction in the sorbent is calculated at the different pH values for

plotting metal loading areas. At pH close to 5.5, Ga(III) represents more than 90% of metal load on PAO/SiO₂. It is remarkable that Ga(III), despite having a very close chemistry to Al(III) (both of them are forming amphoteric hydroxides), is selectively bound to PAO/SiO₂. This is a very interesting property since Al(III) is frequently found in the leachate of ores and industrial effluents (including bauxite leaching in the circulating Bayer liquor). The softness parameters for selected metals follow the order: Ca(II) [−0.66] < Mg(II) [−0.41] < Al(III) [−0.31] < Ga(III) [+0.29] [86]; this may explain the great difference in the sorption behavior of PAO/SiO₂ for these different metal ions. This preference can be also correlated to their first pK_s: Ca(II) [5.2] < Mg(II) [11.5] < Al(III) [14.0] < Ga(III) [37.0] [87]. On the opposite hand, the variation in their hydrated radius does not show a clear trend since Ga(III) [0.62 Å] has a hydrated radius close to the values of Al(III) [0.55 Å] and Mg(II) [0.72 Å] and much lower than for Ca(II) [1.12 Å] [88].

Table AM10 (see Additional Material Section) shows the SEM-EDX analysis of PAO/SiO₂ sorbent after contact with the multi-metal solution at 3 pH values. The weight fraction of Ga element (at the surface of the sorbent) remains in the range 0.39–0.44%. At pH 2.8, all the metal ions are bound to the sorbent (with weight fractions in the range 0.06–0.27%): this is the less selective pH. On the opposite hand, apart Ga(III) at pH 5.9 Al(III) only is significantly bound (weight fraction 0.06%) while at pH 12.8 Mg(II) is the only other metal loaded on PAO/SiO₂. This is consistent with the trends observed in Fig. 12.

3.2.6. Application to the treatment of circulating Bayer liquor

The chemical composition of the Bayer liquor is reported on Table AM4 (see Additional Material Section). Among the 65 analyzed elements, the concentration of 31 metal ions exceeds 10 mg L⁻¹. The solution is very alkaline: the original pH is close to 14. The huge amount of Al(III) (i.e., about 35 g L⁻¹) make the solution very complex (with levels of concentrations of iodide, tungsten, sulfur and phosphorus elements exceeding several grams per liter). Gallium is the tenth element in concentration; with a level of 180 mg Ga L⁻¹. Bayer liquor is usually considered the main source of Ga extraction for commercial applications.

The Bayer liquor was directly tested for Ga(III) recovery using PAO/SiO₂. However, two additional tests were also performed on solutions whose pH was controlled to 11.3 and 11 (taking into account that the original pH was close to 14). The pH control induces a strong precipitation: the precipitate, mainly constituted of aluminum hydroxide

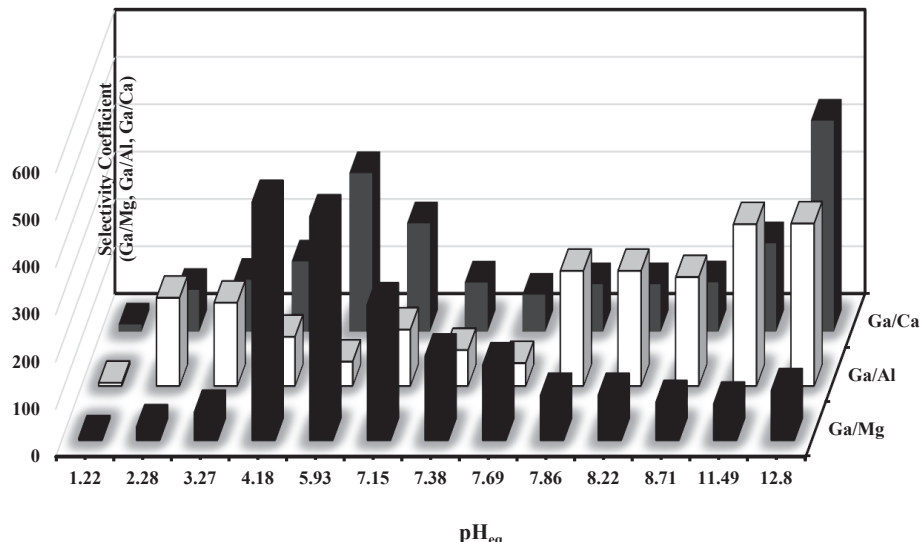


Fig. 12. Ga(III) sorption on PAO/SiO₂ from multi-metal solutions – Selectivity coefficients in function of equilibrium pH (SD: 0.825 g L⁻¹; C_0 : 1.8 (± 0.2) mmol L⁻¹ for Ca(II), Mg(II) and Al(III); 1.01 mmol L⁻¹ for Ga; pH₀: 1.0–13.0; contact time: 6 h; T: 22 ± 1 °C).

and carbonates, appears below pH 11.5 and the amount of produced precipitate increases with decreasing the pH (Table AM11, see [Additional Material Section](#)). The main elements semi-quantitatively analyzed in the precipitate are Al, Na, Mg, Si and Ca, while the precipitation of Ga is negligible. This is confirmed by the ICP-AES analysis of the supernatants (treated effluents after filtration) as appearing in [Table 7](#). The precipitation steps maintain high levels of aluminum, tungsten, and silica.

Sorption experiments were compared for the three solutions (original pH; i.e., pH 14) and after pH control at pH 11.3 and 11. [Table 7](#) shows that, at pH 13.7, the sorbents (i.e.; LSC-600 and PAO/SiO₂) have roughly the same sorption capacities for Al(III), Si(IV), Ca(II), Mg(II) and Cu(II); LSC-600 binds higher amounts of W(V), V(V), Zn(II) and Fe (II,III), while PAO/SiO₂ is more efficient for Ga(III) recovery. At pH 11.3, the sorption capacities of the composite sorbent are maintained for Ga(III), W(V), Si(IV), V(V), while for the other metal ions the sorption capacities decrease. Decreasing the pH to 11 contributes to decrease the sorption capacities of all the metal ions except for Al(III) and for Ga(III) (the sorption capacities are increased from 15 to 21 mg Ga g⁻¹).

The selectivity coefficients are calculated (Figure AM 10, see [Additional Material Section](#)). The highest selectivity coefficients are obtained after controlling the pH to 11–11.3; it is noteworthy that values as high as 318 and 422 can be achieved against Al(III), despite a huge excess of this metal compared to Ga(III). This is consistent with the results reported in [Fig. 12](#). PAO/SiO₂ sorbent has also a remarkable selectivity for Ga(III) against W(V) and Si(IV) close to 135–138 and to a lesser extent to Zn(II) (about 59) when the pH is controlled to 11. The selectivity of the sorbent is decreased at higher pH values. However, at

the original pH of the Bayer liquor (i.e., pH 13.7) the levels of Ga(III) selectivity coefficients are higher for PAO/SiO₂ compared to LSC-600 commercial resin, at least for Al(III), W(V) and Si(IV).

Table AM12 (see [Additional Material Section](#)) shows the SEM observations of the sorbents after being in contact with the Bayer liquor at selected pH values and the EDX analysis of their surface. At pH 13.7 several elements can be identified on both LSC-600 and PAO/SiO₂ sorbents. The pre-treatment of the Bayer liquor at pH 11.3 and better at pH 11 allows the binding of alternative metals and Ga is the most representative metal immobilized on PAO/SiO₂ sorbent (complementary evidence of sorbent selectivity for Ga(III) at this pH).

Taking into account the selectivity coefficients and the sorption capacities, it seems that the pre-treatment of the Bayer liquor at pH 11 allows (a) precipitating limited amounts of valuable metals, (b) maintaining appreciable sorption capacities for Ga(III), and (c) reaching high selectivity coefficients against the most abundant metals.

4. Conclusion

The deposition of poly(acrylonitrile) at the surface of silica particles and the further functionalization of nitrile groups (converted into amidoxime functions) allows preparing a very efficient sorbent for Ga (III) recovery from acidic and alkaline solutions. FTIR and XPS analyses confirm the chemical modification of the sorbent and allow identifying the contribution of amine and hydroxyl groups (on the amidoxime moiety) in metal binding.

The optimum pH for Ga(III) sorption is close to 5.5 at low metal concentration. To prevent metal precipitation at higher concentration, sorption performances were investigated at pH 4. The composition of

Table 7

Evolution of the concentration of major metal ions in the solution at the different steps in the pre-treatment (initial concentration, residual concentrations after precipitation at pH 11.3 and 11), loss percentage during precipitation steps and sorption capacities for PAO/SiO₂ sorbent (as a comparison the sorption is also carried out at pH 13.7 with LSC-600 commercial resin).

Metal	C ₀ (mg L ⁻¹)	Precipitation step					Sorption step			
			Residual concentration (mg L ⁻¹) after precipitation		Loss after precipitation (%)		Sorption capacity (mg metal g ⁻¹)			
			pH 11.3	pH 11	pH 11.3	pH 11	LSC-600	PAO/SiO ₂	PAO/SiO ₂	PAO/SiO ₂
Al	35,000	27,100	15,000	22.57	57.14	20	16	7.2	7.8	
W	2900	2560	2510	11.72	13.45	14	5	4.8	3	
Si	560	510	490	8.93	12.5	6	5	6.6	0.6	
Ca	98	80	76	18.37	22.45	10	10	4.2	1.2	
V	96	82	79	14.58	17.71	11	4	3.6	2.46	
Ga	180	165	162	8.33	10	6	15	15.6	21	
Mg	5.7	5	4.9	12.28	14.04	2.6	2.9	0.24	0.24	
Fe	15	13	13.8	13.33	8	4.4	2.1	1.26	1.548	
Zn	23	22	21.5	4.35	6.52	4.8	1.2	0.3	0.06	
Cu	5	4.5	4.2	10	16	1.1	0.8	0.12	0.06	

Metal	C ₀ (mg L ⁻¹)	Precipitation step					Sorption step			
			Residual concentration (mg L ⁻¹) after precipitation		Loss after precipitation (%)		Sorption efficiency (%)			
			pH 11.3	pH 11	pH 11.3	pH 11	pH 13.7	pH 11.3	pH 11	
Al	35,000	27,100	15,000	22.57	57.14	0.1	0.0	0.0	0.1	
W	2900	2560	2510	11.72	13.45	0.5	0.2	0.3	0.2	
Si	560	510	490	8.93	12.5	1.1	0.9	2.2	0.2	
Ca	98	80	76	18.37	22.45	10.2	10.2	8.8	2.6	
V	96	82	79	14.58	17.71	11.5	4.2	7.3	5.2	
Ga	180	165	162	8.33	10	3.3	8.3	15.8	21.6	
Mg	5.7	5	4.9	12.28	14.04	45.6	50.9	8.0	8.2	
Fe	15	13	13.8	13.33	8	29.3	14.0	16.2	18.7	
Zn	23	22	21.5	4.35	6.52	20.9	5.2	2.3	0.5	
Cu	5	4.5	4.2	10	16	22.0	16.0	4.4	2.4	

(Experimental conditions: T: 22 ± 2 °C; SD: 1 g L⁻¹ for experiments at pH 13.7; and 1.67 g L⁻¹ for experiments at pH 11.3 and 11; contact times: 6 h).

the solution (illustrated by the use of different matrices) significantly influences sorption properties and the maximum sorption capacity may reach up to 2–2.5 mmol Ga(III) g⁻¹, under the most favorable conditions. The sorption isotherms are efficiently modelled by the Langmuir equation for “simple” solutions; however, in the case of complex solutions having high salinity, the unfavorable sorption at low metal concentration makes the Langmuir failing to describe the experimental profile and the Sips equation is more appropriate. Similar trend is observed at pH 13.7. The evaluation of thermodynamic parameters shows that the sorption is endothermic, spontaneous and contributes to increasing the randomness of the sorbent/sorbate system. The equilibrium of sorption is reached within 1 h of contact (under selected experimental conditions) and both the resistance to intraparticle diffusion equation (Crank equation) and the pseudo-first order rate equation successfully fit experimental profiles. Metal desorption can be operated using 1.5 M HCl solutions and the sorption and desorption properties are maintained over 5 cycles (with limited decrease in performances).

In preliminary experiments, the sorbent was efficiently tested for the recovery of Ga(III) from Bayer liquor. Controlling the pH to 11 allows the selective recovery and separation of Ga(III) against major elements such as Al(III), Si(IV) and W(V). The global performance of this material deserves complementary experimentations for application in the valorization of Ga(III) and other metals present in this type of effluent that could actually be considered an important secondary resource of valuable metals.

Acknowledgments

This work was supported by the Science and Technology Major Project of Guangxi (AA 17204100) (China). The authors acknowledge the China Science and Technology Exchange Center (CSTEC) through Talented Young Scientist Program (TYSP) for the post-doc fellowship (teaching assistant position) of Mohammed F. Hamza at School of Resources, Environment and Materials. Authors also thank the technical support of Khalid A.M. Salih and Jie Li, MSc students (with M.F. Hamza as one of the supervisor), at Innovation Center for Metal Resources Utilization and Environment Protection (Guangxi University).

Appendix A. Supplementary material

Supplementary data to this article can be found online at <https://doi.org/10.1016/j.cej.2019.02.094>.

References

- [1] W.A. Breeman, J.M. De, B.E. De, B.F. Bernard, M. Konijnenberg, E.P. Krenning, Radiolabelling DOTA-peptides with 68Ga, *Eur. J. Nucl. Med. Mol. Imaging* 32 (2005) 478–485.
- [2] M.A. Contreras, B. Egaas, K. Ramanathan, J. Hiltner, A. Swartzlander, F. Hasoon, R. Noufi, Progress toward 20% efficiency in Cu(In, Ga)Se₂ polycrystalline thin-film solar cells, *Prog. Photovoltaics Res. Appl.* 7 (1999) 311–316.
- [3] J.L. Marshall, V.R. Marshall, Rediscovery of the elements: Gallium, *Unt Scholarly Works* (2002).
- [4] U.K. Mishra, P. Parikh, Y.F. Wu, AlGaN/GaN HEMTs – an overview of device operation and applications, *Proc. IEEE* 90 (2002) 1022–1031.
- [5] J. Wang, Production processes and uses of gallium, *Sichuan Nonferrous Met.* (2003).
- [6] J. Polednick, Speciation of scandium and gallium in soil, *Chemosphere* 73 (2008) 572–579.
- [7] L.A. Haas, R.D. Weir, Hydrometallurgy of copper, its byproducts and rarer metals, in: L.A. Haas, R.D. Weir (Eds.), *Dallas Symposium of the AIME, Society of Mining Engineers of the AIME, Dallas, USA, 1982*, p. 113.
- [8] Z. Zhao, Y. Yang, Y. Xiao, Y. Fan, Recovery of gallium from Bayer liquor: a review, *Hydrometallurgy* 125 (2012) 115–124.
- [9] M.P. Chen, T.E. Graedel, The potential for mining trace elements from phosphate rock, *J. Cleaner Prod.* 91 (2015) 337–346.
- [10] Z. Zhao, X. Li, Y. Chai, Z. Hua, Y. Xiao, Y. Yang, Adsorption performances and mechanisms of amidoxime resin toward gallium(III) and vanadium(V) from Bayer liquor, *ACS Sustainable Chem. Eng.* 4 (2016) 53–59.
- [11] M.Y. Yang, J. Cai, Study of the chelated resin in the gallium recovery process by the ion exchange method, *Light Met.* 35 (2007) 14–16.
- [12] J. Helgorsky A. Leveque Process for liquid/liquid extraction of gallium, in Google Patents, 1976.
- [13] G.V.K. Puvvada, Liquid–liquid extraction of gallium from Bayer process liquor using Kelex 100 in the presence of surfactants, *Hydrometallurgy* 52 (1999) 9–19.
- [14] A.W. Trochimczuk, E.P. Horwitz, S.D. Alexandratos, Complexing properties of diphenox, a new chelating resin with diphosphonate ligands, toward Ga(III) and In (III), *Sep. Sci. Technol.* 29 (1994) 543–549.
- [15] U. Schilde, H. Kraudelt, E. Uhlemann, U. Gohlke, Selectivity of amidoxime polymers for the sorption of gallate, *Sep. Sci. Technol.* 30 (1995) 2245–2250.
- [16] F.A. Alakras, K. Abu Dari, M.S. Mubarak, Synthesis and chelating properties of some poly(amidoxime-hydroxamic acid) resins toward some trivalent lanthanide metal ions, *J. Appl. Polym. Sci.* 97 (2005) 691–696.
- [17] M.F. Hamza, A.A.H. Abdel-Rahman, E. Guibal, Magnetic glutamine-grafted polymer for the sorption of U(VI), Nd(III) and Dy(III), *J. Chem. Technol. Biotechnol.* 93 (2018) 1790–1806.
- [18] K.S. Rao, D. Sarangi, P.K. Dash, G.R. Chaudhury, Preferential extraction of Ga from Bayer liquor using ion exchange chelating resin containing hydroxamic acid functional group, *J. Chem. Technol. Biotechnol.* 78 (2010) 555–561.
- [19] K. Khunathai, Y. Xiong, B.K. Biswas, B.B. Adhikari, H. Kawakita, K. Ohto, K. Inoue, H. Kato, M. Kurata, K. Atsumi, Selective recovery of gold by simultaneous adsorption-reduction using microalgal residues generated from biofuel conversion processes, *J. Chem. Technol. Biotechnol.* 87 (2012) 393–401.
- [20] D. Wu, L. Zhang, L. Wang, B. Zhu, L. Fan, Adsorption of lanthanum by magnetic alginate-chitosan gel beads, *J. Chem. Technol. Biotechnol.* 86 (2011) 345–352.
- [21] Y. Wang, X.J. Ma, Y.F. Li, X.L. Li, L.Q. Yang, L. Ji, Y. He, Preparation of a novel chelating resin containing amidoxime-guanidine group and its recovery properties for silver ions in aqueous solution, *Chem. Eng. J.* 209 (2012) 394–400.
- [22] Y. Kataoka, M. Matsuda, H. Yoshitake, Y. Hirose, Method for recovery of gallium, in Google Patents, 1984.
- [23] P.A. Riveros, Recovery of gallium from bayer liquors with an amidoxime resin, *Hydrometallurgy* 25 (1990) 1–18.
- [24] R. Liu, Y. Wei, Y. Xu, S. Usuda, S. Kim, H. Yamazaki, K. Ishii, Evaluation study on properties of iso hexyl-BTP/SiO₂-P resin for direct separation of trivalent minor actinides from HLLW, *J. Radioanal. Nucl. Chem.* 292 (2012) 537–544.
- [25] S. Usuda, Y. Wei, Y. Xu, Z. Li, R. Liu, S. Kim, Y. Wakui, H. Hayashi, H. Yamazaki, Development of a simplified separation process of trivalent minor actinides from fission products using novel R-BTP/SiO₂-P adsorbents, *J. Nucl. Sci. Technol.* 49 (2012) 334–342.
- [26] X. Wang, S. Ning, Q. Zou, R. Liu, Y. Wei, Adsorption behavior and mechanism of iso butyl-BTP/SiO₂-P adsorbent for Am(III) and Ln(III) in nitrate solution, *J. Radioanal. Nucl. Chem.* 307 (2016) 2001–2008.
- [27] X.P. Wang, S.Y. Ning, R.Q. Liu, Y.Z. Wei, Stability of isoHex-BTP/SiO₂-P adsorbent against acidic hydrolysis and γ -irradiation, *Science China* 57 (2014) 1464–1469.
- [28] Y.Z. Wei, H. Hoshi, M. Kumagai, T. Asakura, Y. Morita, Separation of Am(III) and Cm(III) from trivalent lanthanides by 2,6-bistriazinylpyridine extraction chromatography for radioactive waste management, *J. Alloys Compd.* 374 (2004) 447–450.
- [29] F. Zha, X. Wang, X. Wang, A. Khayambashi, Y. Wei, F. Tang, L. He, Synthesis of a novel silica-based macroporous HNA/SiO₂-P adsorbent and its adsorption behavior for uranium from aqueous solutions, *J. Radioanal. Nucl. Chem.* 311 (2017) 1793–1802.
- [30] S. Ning, X. Wang, R. Liu, Y. Wei, L. He, F. Tang, Evaluation of Me-2-CA-BTP/SiO₂-P adsorbent for the separation of minor actinides from simulated HLLW, *J. Radioanal. Nucl. Chem.* 303 (2015) 2011–2017.
- [31] Y.Z. Wei, M. Yamaguchi, M. Kumagai, Y. Takashima, T. Hoshikawa, F. Kawamura, Separation of actinides from simulated spent fuel solutions by an advanced ion-exchange process, *J. Alloys Compd.* 271–273 (1998) 693–696.
- [32] A. Khayambashi, X. Wang, Y. Wei, Solid phase extraction of uranium (VI) from phosphoric acid medium using macroporous silica-based D₂EHPA-TOPO impregnated polymeric adsorbent, *Hydrometallurgy* 164 (2016) 90–96.
- [33] E.S. Dragan, D.F.A. Loghin, A.I. Cocarta, Efficient sorption of Cu²⁺ by composite chelating sorbents based on potato starch-graft-polyamidoxime embedded in chitosan beads, *ACS Appl. Mater. Interf.* 6 (2014) 16577–16592.
- [34] S.D. Alexandratos, X.P. Zhu, M. Florent, R. Sellin, Polymer-supported bifunctional amidoximes for the sorption of uranium from seawater, *Ind. Eng. Chem. Res.* 55 (2016) 4208–4216.
- [35] G. Bayramoglu, M.Y. Arica, MCM-41 silica particles grafted with polyacrylonitrile: modification in to amidoxime and carboxyl groups for enhanced uranium removal from aqueous medium, *Microporous Mesoporous Mater.* 226 (2016) 117–124.
- [36] T. Arai, Y. Wei, M. Kumagai, K. Horiguchi, Separation of rare earths in nitric acid medium by a novel silica-based pyridinium anion exchange resin, *J. Alloys Compd.* 408–412 (2006) 0–1012.
- [37] Y. Wei, M. Kumagai, Y. Takashima, G. Modolo, R. Odoj, Studies on the separation of minor actinides from high-level wastes by extraction chromatography using novel silica-based extraction resins, *Nucl. Technol.* 132 (2000) 1472–1475.
- [38] W. He, X. Zhou, C. Liu, J. Zhang, C. Huang, The synthesis of macroreticular chelating resins containing amidoxime groups and their properties of recovery of uranium, *Uranium Min. Metall.* 16 (1997) 186–194.
- [39] Y. Xie, J. Wang, M. Wang, X. Ge, Fabrication of fibrous amidoxime-functionalized mesoporous silica microsphere and its selectively adsorption property for Pb²⁺ in aqueous solution, *J. Hazard. Mater.* 297 (2015) 66–73.
- [40] M.V. Lopez-Ramon, F. Stoeckli, C. Moreno-Castilla, F. Carrasco-Marin, On the characterization of acidic and basic surface sites on carbons by various techniques, *Carbon* 37 (2009) 1215–1221.
- [41] H. Chen, A. Wang, Adsorption characteristics of Cu(II) from aqueous solution onto poly(acrylamide)/attapulgite composite, *J. Hazard. Mater.* 165 (2009) 223–231.
- [42] G.E. Rajaei, H. Aghaie, K. Zare, M. Aghaie, Adsorption of Cu(II) and Zn(II) ions from

- aqueous solutions onto fine powder of *Typha latifolia L.* root: kinetics and isotherm studies, *Res. Chem. Intermed.* 39 (2013) 3579–3594.
- [43] Y.S. Ho, G. McKay, Pseudo-second order model for sorption processes, *Proc. Biochem.* 34 (1999) 451–465.
- [44] J. Crank, *The Mathematics of Diffusion*, 2nd ed., Oxford University Press, Oxford, UK, 1975, p. 414.
- [45] K.Y. Foo, B.H. Hameed, Insights into the modeling of adsorption isotherm systems, *Chem. Eng. J.* 156 (2010) 2–10.
- [46] I. Langmuir, The adsorption of gases on plane surfaces of glass, mica and platinum, *J. Amer. Chem. Soc.* 40 (1918) 1361–1402.
- [47] H.M.F. Freundlich, Über die adsorption in lasungen, *Z. Phys. Chem.* 57 (1906) 385–470.
- [48] C. Tien, *Adsorption Calculations and Modeling*, Butterworth-Heinemann, Newton, MA, 1994 243 pp.
- [49] N.V. Duffy, Interpretation of infrared spectra, *J. Chem. Educ.* 49 (1972) 30–45.
- [50] T. Yang, L. Wang, M. Liang, Y. Chen, H. Zou, Cross-linked polyvinyl amidoxime fiber: a highly selective and recyclable adsorbent of gallium from Bayer liquor, *Iran. Polym. J.* 27 (2018) 589–597.
- [51] A.M. Atta, A.A.H. Abdel-Rahman, I.E. El Aassy, F.Y. Ahmed, M.F. Hamza, Adsorption properties of uranium (VI) ions on reactive crosslinked acrylamidoxime and acrylic acid copolymer resins, *J. Dispersion Sci. Technol.* 32 (2011) 84–94.
- [52] M.F. Hamza, J.-C. Roux, E. Guibal, Uranium and europium sorption on amidoxime-functionalized magnetic chitosan micro-particles, *Chem. Eng. J.* 344 (2018) 124–137.
- [53] P. Selvi, M. Ramasami, M.H.P. Samuel, P. Adaikkalam, G.N. Srinivasan, Recovery of gallium from Bayer liquor using chelating resins in fixed-bed columns, *Ind. Eng. Chem. Res.* 43 (2004) 2216–2221.
- [54] A.R. Adel, E.E.A. Ibrahim, Y.A. Fadia, F.H. Mohammed, Studies on the uptake of rare earth elements on polyacrylamidoxime resins from natural concentrate leachate solutions, *J. Dispersion Sci. Technol.* 31 (2010) 1128–1135.
- [55] Z. Zhao, X. Xie, Z. Wang, Y. Tao, X. Niu, X. Huang, L. Liu, Z. Li, Immobilization of *Lactobacillus rhamnosus* in mesoporous silica-based material: An efficiency continuous cell-recycle fermentation system for lactic acid production, *J. Biosci. Bioeng.* 121 (2016) 645–651.
- [56] J. Coates, *Interpretation of Infrared Spectra, A Practical Approach*, in: R.A. Meyers (Ed.), *Encyclopedia of Analytical Chemistry*, John Wiley & Sons Ltd, Chichester, UK, 2000, pp. 10815–10837.
- [57] N. Liu, R.A. Assink, B. Smarsly, C.J. Brinker, Synthesis and characterization of highly ordered functional mesoporous silica thin films with positively chargeable -NH₂ groups, *Chem. Commun.* 9 (2003) 1146–1147.
- [58] X. Zhang, R.F. Guan, D.Q. Wu, K.Y. Chan, Enzyme immobilization on amino-functionalized mesostructured cellular foam surfaces, characterization and catalytic properties, *J. Mol. Catal. B: Enzym.* 33 (2005) 43–50.
- [59] S. Li, W. Wu, H. Li, X. Hou, The direct adsorption of low concentration gallium from fly ash, *Sep. Sci. Technol.* 51 (2016) 395–402.
- [60] H. Long, Z. Zhao, Y. Chai, X. Li, Z. Hua, Y. Xiao, Y. Yang, Binding mechanism of the amidoxime functional group on chelating resins toward gallium(III) in Bayer liquor, *Ind. Eng. Chem. Res.* 54 (2015) 8025–8030.
- [61] M. Bazzar, M. Ghaemy, R. Alizadeh, Synthesis and characterization of new fluorescent polyimides bearing 1,2,4-triazole and 1,2-diaryl quinoxaline: study properties and application to the extraction/elimination of metallic ions from aqueous media, *React. Funct. Polym.* 73 (2013) 492–498.
- [62] T.C. Tsai, D.A. Tree, M.S. High, Degradation kinetics of polyaniline base and sulfonated polyaniline, *Ind. Eng. Chem. Res.* 33 (1994) 2600–2606.
- [63] M. Ajmal, S. Demirci, M. Siddiq, N. Aktas, N. Sahiner, Amidoximated poly(acrylonitrile) particles for environmental applications: removal of heavy metal ions, dyes, and herbicides from water with different sources, *J. Appl. Polym. Sci.* 133 (2016).
- [64] N.A.M. Zahri, S. Jamil, L.C. Abdullah, T.C.S. Yaw, M.N. Mobarekeh, S.J. Huey, N.S.M. Rapeia, Improved method for preparation of amidoxime modified poly(acrylonitrile-co-acrylic acid): characterizations and adsorption case study, *Polymers* 7 (2015) 1205–1220.
- [65] M.H. Beyki, F. Feizi, F. Shemirani, Melamine-based dendronized magnetic polymer in the adsorption of Pb(II) and preconcentration of rhodamine B, *React. Funct. Polym.* 103 (2016) 81–91.
- [66] J.L. Bourque, M.C. Biesinger, K.M. Baines, Chemical state determination of molecular gallium compounds using XPS, *Dalton Trans.* 45 (2016) 7678–7696.
- [67] W.L. Xu, C. Fang, F. Zhou, Z. Song, Q. Liu, R. Qiao, M. Yu, Self-assembly: a facile way of forming ultrathin, high-performance graphene oxide membranes for water purification, *Nano Lett.* 17 (2017) 2928–2933.
- [68] D.P. Depuccio, L. Ruiz Rodríguez, E. Rodriguez Castellon, P. Botella, J.M.L. Nieto, C.C. Landry, Investigating the influence of Au nanoparticles on porous SiO₂-WO₃ and WO₃ methanol transformation catalysts, *J. Phys. Chem. C* 120 (2016) 27954–27963.
- [69] F. Yun, B.J. Hinds, S. Hatatani, S. Oda, Q.X. Zhao, M. Willander, Study of structural and optical properties of nanocrystalline silicon embedded in SiO₂, *Thin Solid Films* 375 (2000) 137–141.
- [70] Y. Zhang, L. Zhu, Y. Wang, Z. Lou, W. Shan, Y. Xiong, Y. Fan, Preparation of a biomass adsorbent for gallium(III) based on corn stalk modified by iminodiacetic acid, *J. Taiwan Inst. Chem. Eng.* 91 (2018) 291–298.
- [71] P. Benerezeth, G.S. Diakonov II, J.L. Pokrovski, J. Dandurand, I.L. Khodakovsky Schott, Gallium speciation in aqueous solution. Experimental study and modelling.2. Solubility of alpha-GaOOH in acidic solutions from 150 to 250 degrees C and hydrolysis constants of gallium (III) to 300 degrees C, *Geochim. Cosmochim. Acta* 61 (1997) 1345–1357.
- [72] A.A.H. Abdel-Rahman, A.M. Atta, I.E. El Aassy, F.Y. Ahmed, M.F. Hamza, Studies on the uptake of uranium(VI) ions on polyacrylamidoxime resins synthesized by free radical polymerization with different crosslinking ratios and pore solvents, *J. Dispersion Sci. Technol.* 32 (2011) 224–234.
- [73] A. Rahmati, A. Ghaemi, M. Samadfam, Kinetic and thermodynamic studies of uranium(VI) adsorption using Amberlite IRA-910 resin, *Ann. Nucl. Energy* 39 (2012) 42–48.
- [74] S.U. Yu-Qin, X.L. Liu, Z.G. Zhang, Synthesis and adsorption behavior of macro-porous amidoxime resin for separate of gallium, *Chin. J. Process Eng.* 10 (2010) 893–898.
- [75] M.F. Hamza, M.G. Mahfouz, A.A.H. Abdel-Rahman, Adsorption of uranium (VI) ions on hydrazinyl amine and 1,3,4-thiadiazol-2(3 H)-thion chelating resins, *J. Dispersion Sci. Technol.* 33 (2012) 1544–1551.
- [76] S. Saber-Samandari, H.O. Gulcan, S. Saber-Samandari, M. Gazi, Efficient removal of anionic and cationic dyes from an aqueous solution using pullulan-graft-poly-acrylamide porous hydrogel, *Water Air Soil Pollut.* 225 (2014) Art. N° 2177.
- [77] D. Ma, B. Zhu, C. Bo, W. Jian, J. Zhang, Fabrication of the novel hydrogel based on waste corn stalk for removal of methylene blue dye from aqueous solution, *Appl. Surf. Sci.* 422 (2017) 944–952.
- [78] C.-H. Lee, H.-Y. Lin, E.I. Cadogan, S.R. Popuri, C.-Y. Chang, Biosorption performance of biodegradable polymer powders for the removal of gallium(III) ions from aqueous solution, *Pol. J. Chem. Technol.* 17 (2015) 124–132.
- [79] J.S. Liu, Z.G. He, J. Cai, C.G. Cai, B.X. Zhou, W.M. Cai, Separation of indium (III), gallium (III), and zinc (II) with Levextrel resin containing di(2-ethylhexyl) phosphoric acid (CL-P204): Part I. Selection of separation conditions, *Rare Met.* 22 (2003) 235–240.
- [80] J.S. Liu, H. Chen, X.Y. Chen, Z.L. Guo, Y.C. Hu, C.P. Liu, Y.Z. Sun, Extraction and separation of In(III), Ga(III) and Zn(II) from sulfate solution using extraction resin, *Hydrometallurgy* 82 (2006) 137–143.
- [81] W.-L. Chou, C.-T. Wang, Y.-H. Huang, Removal of gallium ions from aqueous solutions using tea waste by adsorption, *Fresenius Environ. Bull.* 19 (2010) 2848–2856.
- [82] Z. Zhang, H. Zhang, Y. Hu, X. Yang, S. Yao, Novel surface molecularly imprinted material modified multi-walled carbon nanotubes as solid-phase extraction sorbent for selective extraction gallium ion from fly ash, *Talanta* 82 (2010) 304–311.
- [83] S. Chegrouche, A. Bensmaili, Removal of Ga(III) from aqueous solution by adsorption on activated bentonite using a factorial design, *Water Res.* 36 (2002) 2898–2904.
- [84] L. Zhang, Y. Zhu, H. Li, N. Liu, X. Liu, X. Guo, Kinetic and thermodynamic studies of adsorption of gallium(III) on nano-TiO₂, *Rare Met.* 29 (2010) 16–20.
- [85] T.K. Mukherjee, S.P. Chakraborty, A.C. Bidaye, C.K. Gupta, Recovery of pure vanadium-oxide from bayer sludge, *Miner. Eng.* 3 (1990) 345–353.
- [86] Y. Marcus, *Ion Properties*, Marcel Dekker Inc, New York, NY, 1997, p. 259.
- [87] C.F. Baes Jr., R.E. Mesmer, *Hydrolysis of Cations*, Wiley, NY, 1976.
- [88] I. Persson, Hydrated metal ions in aqueous solution: how regular are their structures? *Pure Appl. Chem.* 82 (2010) 1901–1917.